AIAA JOURNAL
Vol. 50, No. 8, August 2012

Turbine Burners: Performance Improvement and Challenge of Flameholding

W. A. Sirignano, D. Dunn-Rankin, F. Liu, B. Colcord, and S. Puranam
University of California, Irvine, Irvine, California 92697

DOI: 10.2514/1.J051562

Nomenclature

A	=	preexponential chemical rate constant
a, b	=	mass fraction exponents in chemical rate law
C	=	correction factor
D	=	cavity depth
E	=	activation energy
f	=	frequency
h	=	enthalpy
L	=	cavity length
M	=	Mach number, mixedness parameter
n	=	Rossiter mode number
p	=	pressure
Q	=	fuel heating value
R	=	universal gas constant
Re	=	Reynolds number
St	=	Strouhal number
T	=	temperature
t	=	time
U	=	flow velocity over cavity
x	=	position along mixing layer
Y	=	mass fraction
y	=	transverse position in mixing layer
γ	=	ratio of specific heats
η	=	burning efficiency
κ	=	ratio of convective velocity of vorticity to freestream velocity
ξ	=	Rossiter variable
ρ	=	density
ω	=	chemical reaction rate

Subscripts

C	=	carbon
F	=	fuel
N	=	nitrogen
O	=	oxygen

I. Introduction

GAS-turbine-engine designers want to increase the thrust-to-weight ratio and to widen the range of engine operation. One major consequence of such improvements is that the residence time in the primary combustor can become shorter than the time required

William A. Sirignano serves as Professor of Mechanical and Aerospace Engineering and occupies the Henry Samueli Endowed Chair in Engineering at the University of California, Irvine (UCI). His undergraduate education was at Rensselaer Polytechnic Institute with doctoral education at Princeton University. He has served as Dean, School of Engineering, UCI; George Tallman Ladd Professor and Department Head of Mechanical Engineering, Carnegie-Mellon University; and Professor, Princeton University. His major research and teaching interests include spray combustion, turbulent combustion, aerospace propulsion, fluid dynamics, and applied mathematics. He has authored or coauthored almost 500 research papers and given about 300 research seminars and presentations. Dr. Sirignano's awards and recognitions include National Academy of Engineering membership; Fellow status in the AIAA, American Society of Mechanical Engineers, American Association for the Advancement of Science, American Physical Society, and SIAM; AIAA Propellants and Combustion Award; ASME Freeman Scholar Fluids Engineering Award; AIAA Pendray Aerospace Literature Award; The Combustion Institute Alfred C. Egerton Gold Medal; Institute for the Dynamics of Explosions and Reactive Systems (IDERS) Oppenheim Award; AIAA Energy Systems Award; AIAA Wyld Propulsion Award; and AIAA Sustained Service Award.

Derek Dunn-Rankin is Professor and current Chair in the Department of Mechanical and Aerospace Engineering at the University of California, Irvine (UCI). He received his Ph.D. degree (1985) from the University of California, Berkeley, with an emphasis in combustion science. He was a Postdoctoral Researcher at Sandia National Laboratories Combustion Research Facility until 1987, when he joined the faculty of Mechanical Engineering at UCI. Dr. Dunn-Rankin's research is primarily in combustion and energy, droplets and sprays, and applications of laser diagnostic techniques to practical engineering systems, with recent emphasis on miniature combustion systems and electrical aspects of flames. He has more than 300 technical publications and presentations in these fields, and he is a Board officer of both the International Combustion Institute and the Institute for the Dynamics of Explosions and Reactive Systems. Professor Dunn-Rankin is currently the Faculty Director for CAMP, the California Louis Stokes Alliance for Minority Participation, a program designed to increase minority representation in science and technology. He received a National Science Foundation Presidential Young Investigator Award in 1989, the Society of Automotive Engineering Ralph R. Teetor Engineering Educator Award in 1991, a Fulbright Scholar Fellowship in 1997, and a Japan Society for the Promotion of Science Fellowship in 2008.

Presented at the 45th AIAA Joint Propulsion Conference, Denver, CO, 3–6 August 2009; received 17 August 2011; revision received 4 December 2011; accepted for publication 18 December 2011.

for complete combustion. Combustion would then extend into the turbine passage, which is troublesome at first sight, because it can lead to an increase in heat transfer challenges. However, a significant benefit can result from augmented burning in the turbine. Sirignano and Liu [1] have shown by thermodynamic analysis that augmented combustion in the aircraft turbojet engine allows for 1) a reduction in afterburner length and weight, 2) a reduction in specific fuel consumption compared with afterburner engines, and 3) an increase in specific thrust, compared with an engine with no augmenter. The increase in specific thrust implies that larger thrust can be achieved with the same engine cross section or that the same thrust can be achieved with a smaller cross section (and, therefore, still-smaller weight). A turbine burner might also make possible turbomachinery stages without reducing thrust or increasing fuel consumption substantially. Similarly, for ground-based engines, turbine-burner benefits have been shown by thermodynamic analysis to occur in power/weight and efficiencies [1].

There are various options for location of an augmentative combustor. The original study in [1] refers to the continuous-turbine-burner concept (CTB), in which combustion continues in the stator and rotor. An option to avoid complications with burning in a stator or rotor stage is the interturbine-burner (ITB) concept [2]. For example, one possibility is to use the transition duct between the high-pressure and low-pressure turbine stages. Another intermediate possibility is to use the turbine stator (nozzle) passages as combustors (one combustor between each set of vanes). One consequence of the latter choice is that significant acceleration of the flow would occur while mixing and reaction are underway. A third hybrid choice is that both the transition duct and the first stator (turbine nozzles) in the low-pressure turbine would serve as the combustion chamber. That is, combustion processes would begin in the transition duct but extend into the stators. All options require compact combustors, i.e., small size, with associated reductions in residence time.

To take advantage of a combustor in the stators, it is necessary to address some fundamental combustion and fluid dynamic challenges. The compressible, turbulent flow through the turbine passages accelerates in the streamwise direction while experiencing a transverse acceleration associated with the turning of the flow. Each of these accelerations can reach 10^5 g [1]. The flow accelerates from subsonic speeds to supersonic speeds in a very short distance. Therefore, flameholding is a challenge. Temperature, density, and species concentration gradients occur in this flow, due to the addition of fuel, mixing, and combustion. The transverse acceleration of the stratified mixture can result in hydrodynamic instabilities that might significantly affect energy conversion rates, heat transfer rates to the turbomachinery, force loading on the turbine blades, and the character of the turbulent flow. Combustion in high-acceleration flows is an important new area of applied scientific research.

To understand some of the issues concerning burning in the passages of the turbine of a turbojet or turbofan engine, it is useful to review some of the research in four relevant areas: thermal-cycle analysis, reacting mixing layers in accelerating flows, flameholding in high-speed flows, and compact continuous combustors.

II. Thermal-Cycle Analysis

Figure 1 shows a schematic for a representative turbofan jet engine. The main combustor is located between stations 3 and 4. Three possible locations are shown for the augmenter: the classical afterburner can be placed between stations 5 and 6; fuel can be added to the secondary bypass airstream with the burner between stations $3f$ and $4f$; and a burner can be imbedded in the turbine between positions 4 and 5. Here, we focus on this last choice: namely, the turbine burner.

In Fig. 2, the temperature–entropy plot gives a comparison of the thermal cycle between a turbojet engine with an afterburner and the engine with both an afterburner and an idealized (i.e., constant-temperature) continuous turbine burner. The constant temperature through the turbine stages implies that combustion heat is added at the same rate as work is done on the turbine; clearly, this is an idealized description, but the cycle comes closer to the Carnot cycle, resulting in higher thermal efficiency and at the same time providing higher specific power or specific thrust because of the additional fuel burn per unit core engine mass flow rate.

Feng Liu is a Professor in the Department of Mechanical and Aerospace Engineering at the University of California, Irvine (UCI). He received his B.S. degree from the Department of Jet Propulsion of Northwestern Polytechnical University and his Ph.D. degree from Princeton University in 1991 before joining the faculty of Mechanical and Aerospace Engineering at UCI. Dr. Liu's research is in computational fluid dynamics and combustion, aerodynamics, and jet propulsion. He has authored or coauthored more than 150 journal and conference papers in these fields. Professor Liu is an Associate Fellow of the AIAA and currently serves as Associate Editor for the *Journal of Propulsion and Power*, Member of the Editorial Board of the *Journal of Computational Fluid Dynamics*, and Member of the Editorial Board of *Acta Mechanica Sinica*. He received a NASA Summer Faculty Fellowship in 2001 and the title of Changjiang Visiting Distinguished Professorship from the Chinese Ministry of Education in 2005.

Ben Colcord is a Postdoctoral Researcher at Georgia Institute of Technology. He received a B.E. degree from the University of Auckland in 2002 and M.S. and Ph.D. degrees from the University of California, Irvine, in 2007 and 2011, respectively, where he was also a Graduate Student Researcher. Dr. Colcord's primary research interests are in computational fluid dynamics and combustion.

Srivatsava Puranam is a Postdoctoral Researcher at the Combustion Research Facility of Sandia National Laboratories, where he is studying combustion phasing control using variable valve techniques in an automotive-scale charge compression ignition engine. He received his B.S. degree from the Indian Institute of Technology Bombay in 2004, M.S. degree from the University of Toronto in 2006, and Ph.D. degree from the University of California, Irvine, in 2010. Dr. Puranam's research interests are in gas turbine and internal-combustion engines.

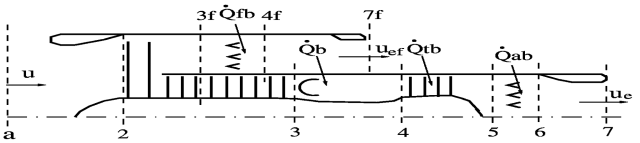

Fig. 1 Schematic for turbofan engine and possible combustor locations.

The turbine-burner concept [1] at first involved continuous burning in the turbine. An extended concept includes not only continuous burning in the turbine, but also discrete interstage turbine burners as an intermediate option [2]. Figure 3 shows the concept for the interturbine burner. In Figs. 3b–3d, we see augmentative combustors between consecutive turbine stages. Between the stages, fuel injection and burning lead to a monotonically increasing temperature in that region, immediately followed by a sharp temperature decrease through the turbine stage. In examining Fig. 3d, we see that as the number of burners goes to infinity, the continuous-combustion (constant-temperature) burner of Fig. 3a is approached asymptotically.

We can consider a few turbine configurations that differ in some aspects, but are still described thermodynamically in Fig. 3. The interstage burner would have combustion occurring between the rotor of an upstream stage and the stator of the downstream stage. The portions of the diagram in Figs. 3b–3d with increasing temperature describe the burner; the sharp temperature drop at constant or near-constant entropy pertains to the turbine stage (nozzle and rotor), where thermal energy is converted to work. Another interpretation that motivates our research is that the combustion is occurring within the nozzle, which causes an increase in thermal energy, while some of that thermal energy is converted to kinetic energy. Then the temperature drops sharply in the downstream portion of the stator and the rotor, where thermal energy is again converted to kinetic energy and the kinetic energy is then converted to work. In the ideal situation, combustion would occur in both the stator and rotor portions of each stage, with addition rates balancing the rates for conversion to kinetic energy and work so that temperature remains constant through all stages. The configuration that combines the combustor with at least a portion of the turbine stage should produce an engine of smaller size and weight. So our research has focused on the integration of the burner with the turbine nozzle. We leave for future research the combination of the burner with the rotating portion, i.e., the CTB concept.

A detailed cycle analysis has been made on the performance of turbojet and ground-based gas-turbine engines with combustion in the turbine. Instead of using idealized cycles, component efficiencies based on typical engines were used. It was found that the performance gains of the continuous turbine burner over a conventional engine based on idealized cycles still stand when more

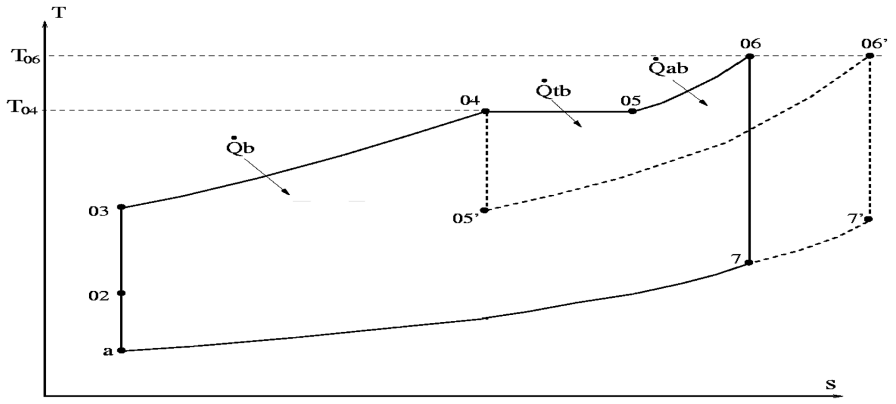

Fig. 2 Thermal descriptions of two configurations: classical afterburner (solid-and-dashed-line path) and ideal turbine burner with afterburner (all-solid-line path). Temperature is plotted versus entropy.

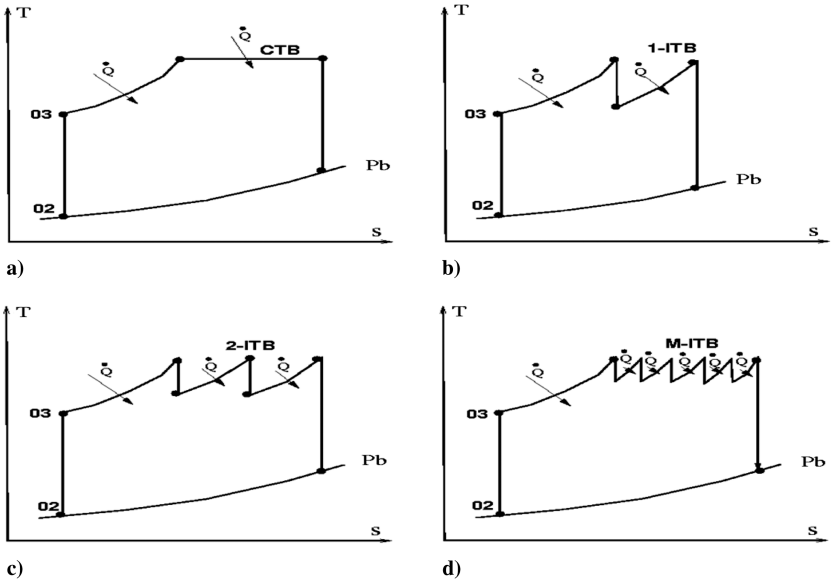

Fig. 3 Thermal-cycle comparison for turbojet engines with no afterburner. Four cases are shown: a) constant-temperature turbine burner, b) one ITB, c) two ITBs, and d) multi-interturbine burner.

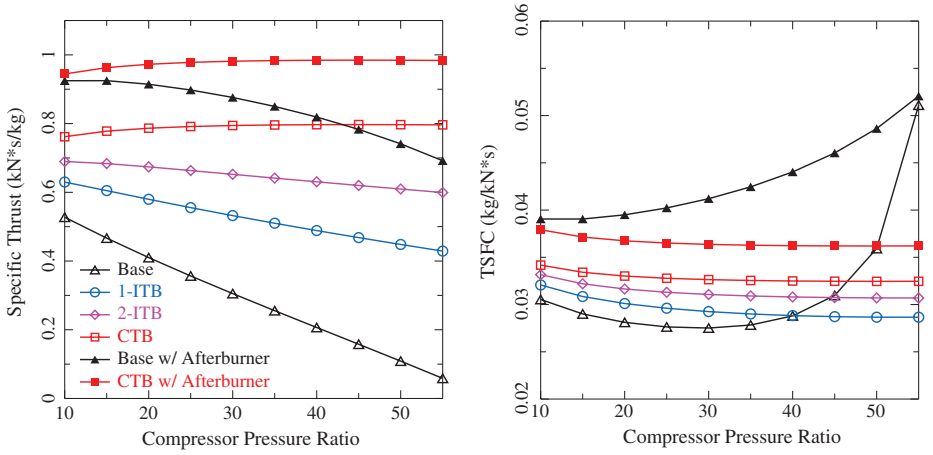

a) b)

Fig. 4 Specific thrust and specific fuel consumption as a function of compression ratio are compared for various combustor configurations.

realistic component efficiencies are included. In fact, the turbine-burner configurations appear even more beneficial for realistic engines than for idealized engines, especially at high compressor compression ratios and higher flight Mach numbers. This occurs because the turbine burner has the advantage of providing sufficient power to drive the compressor with less stagnation pressure drop across the turbine stages. The detailed analysis, computational results and discussions were presented in [1]. Some results follow.

Figure 4 shows performance comparisons among the different configurations for varying pressure ratios at the flight Mach number $M = 2.0$ with maximum allowable turbine inlet temperature $T_{04} = 1500$ K and maximum afterburner temperature $T_{06} = 1900$ K. The turbine power ratios are fixed at 40:60 and 33:33:34 for the 1-ITB and 2-ITB engines, respectively.

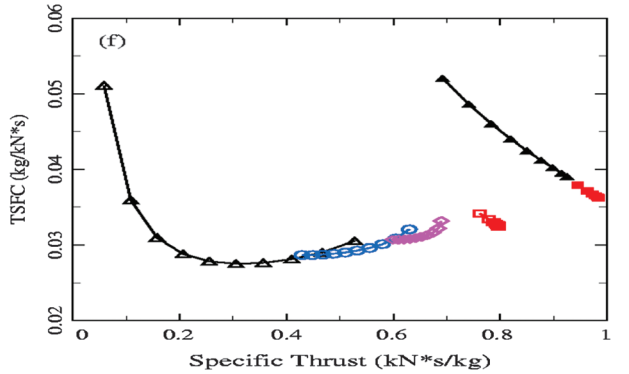

Fig. 5 Specific fuel consumption vs specific thrust for various combustor configurations.

As shown in Fig. 4, the turbine burner produces more thrust than an engine without an augmenter, but at the cost of increased fuel consumption for current compressor ratio values. At the higher compressor ratio values projected for the future, the turbine burner is superior in both thrust and fuel consumption. More thrust and higher fuel consumption occurs as more turbine burners are employed. The engine with afterburner produces more thrust, but consumes significantly more fuel, compared with both the conventional and the turbine-burner engines. The advantage of the turbine-burner engines in both fuel consumption and thrust levels over the afterburner becomes greater at the high compression ratios, with the turbine burner providing comparable (or even more) thrust at a much reduced fuel consumption rate. The engine with both afterburner and turbine burner is superior to the afterburner engine in both thrust and fuel consumption for all pressure ratios explored. Figure 5 gives the same data from Fig. 4 as a plot of specific fuel consumption versus specific thrust with compressor ratio as a running parameter along the curves. Clearly, turbine-burner engines are able to provide significantly higher specific thrust at almost the same specific fuel consumption rate as that of a conventional engine without afterburner. With the same afterburner, addition of the turbine burner not only increases specific thrust, but also reduces the specific fuel consumption rate.

The results in Fig. 6 show the performance over the flight Mach number range up to 2.5 at a fixed compression ratio of 40. The qualitative effect of Mach number is identical to that of compressor ratio. Below a Mach number of about 2, the turbine burner produces more thrust than an engine without augmenter, but at the cost of

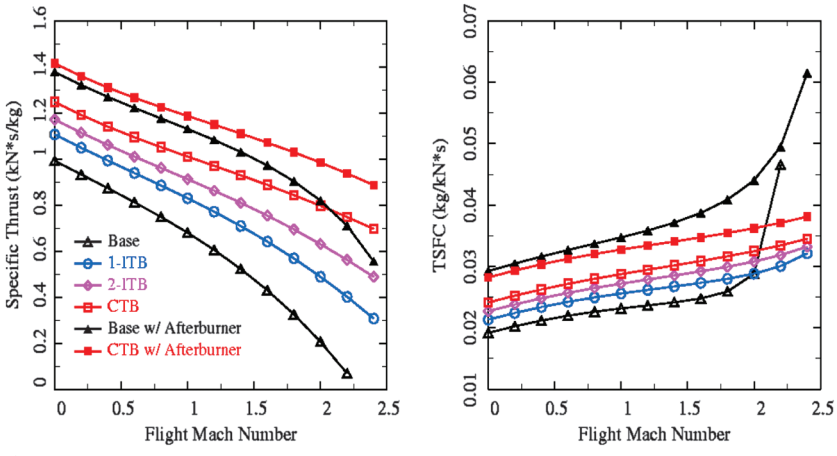

a) b)

Fig. 6 Specific thrust and specific fuel consumption as a function of flight Mach number are compared for various combustor configurations.

increased fuel consumption. At higher-Mach-number values, the turbine burner is superior in both thrust and fuel consumption. The engine with afterburner provides more thrust, but consumes more fuel for much of the Mach number range. At the higher Mach numbers, the turbine burner becomes even more superior in fuel consumption and competitive or slightly better on thrust compared with the afterburner engine.

The above analysis for turbojet engines was further extended to include turbofan engines [2]. Thermodynamic cycle analyses were performed to compare the relative performances of the conventional engine and the turbine-burner engine with different combustion options for both turbojet and turbofan engines. Turbine-burner engines are shown to provide significantly higher specific thrust with no or only small increases in thrust specific fuel consumption compared with conventional engines. Turbine-burner engines also widen the operational ranges for flight Mach number and compressor pressure ratio. The performance gain of turbine-burner engines over conventional engines increases with compressor pressure ratio, fan bypass ratio, and flight Mach number. See [2] for more detail on the analysis.

Figures 7a and 7b compare the performances as functions of Mach number of a sample continuous-turbine-burner (CTB) engine, several discrete ITB engines, and the conventional turbofan engines with inlet temperature of 1500 K and (if used) afterburner temperature of 1900 K. These figures show that the turbine-burner engines are far superior to their base engine counterparts. The conventional turbofan engines are optimal at relatively lower compression ratios and bypass ratios, while the turbine-burner engines favor higher compression and bypass ratio, as discussed in detail in [2]. The comparisons made in Fig. 7 are between the conventional turbofan engines with compressor pressure ratio of 30, fan pressure ratio of 1.65, and bypass ratio of 8 and the turbine-burner engines with compressor pressure ratio of 60, fan pressure ratio of 1.75, and bypass ratio of 12. The 1-ITB engine provides about 50% increase in specific thrust (based on core engine mass flow rate) over the base engine, even more than the thrust of the base engine with the afterburner, while its specific fuel consumption rate is lower than or equal to that of the base engine without the afterburner for the entire subsonic flight range. At Mach number 1, the 2-ITB engine produces 80% more specific thrust while incurring only about 10% increase in specific fuel consumption rate; the CTB engine is capable of producing 120% more thrust with about 15% increase in specific fuel consumption rate compared with the base engine. More significantly, the 2-ITB and the CTB engines are capable of operating over the entire 0 to 2 flight Mach range. The conventional base engines cannot operate beyond Mach 1.25. Figure 8 shows performance of various turbofan configurations as a function of fan bypass ratio at a flight Mach number of 0.87. At high bypass ratios projected for the future, the turbine-burner engine surpasses the afterburner engine in thrust and becomes competitive with the nonaugmented engine in fuel consumption.

The thermodynamic cycle for a ground-based turbine-burner engine without heat regeneration when compared with a conventional gas-turbine engine gives a dramatically larger specific

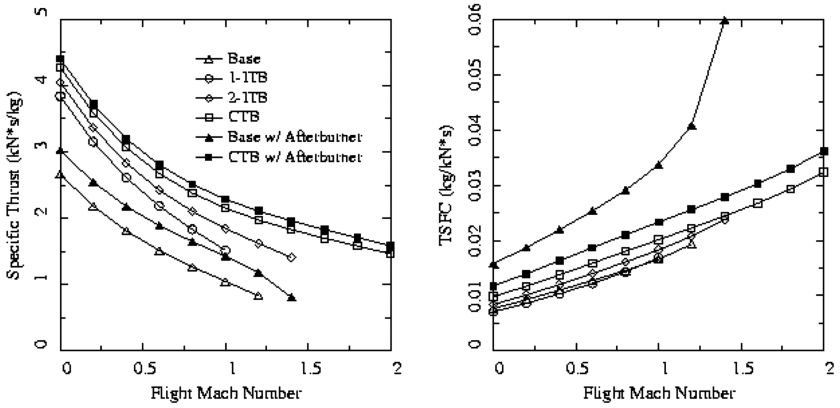

a) b)

Fig. 7 Performance of turbofan engines as a function of flight Mach number.

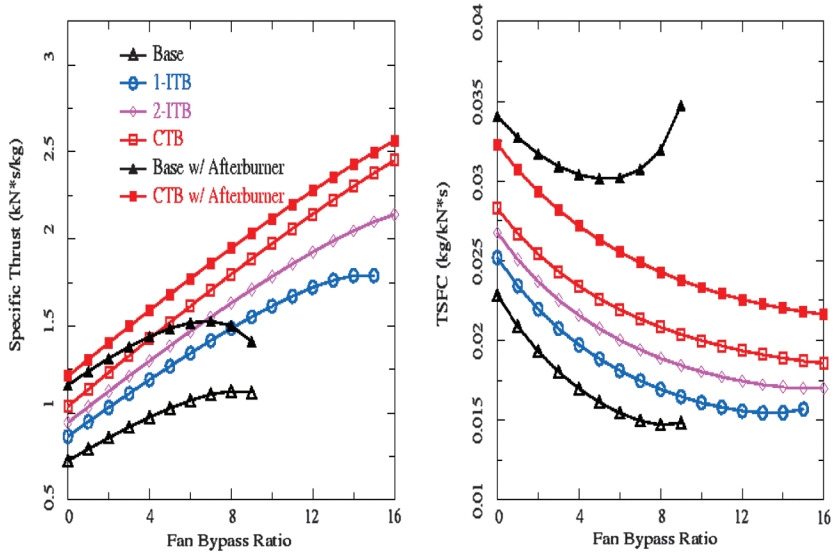

a) b)

Fig. 8 Performance of turbofan engines as a function of fan bypass ratio.

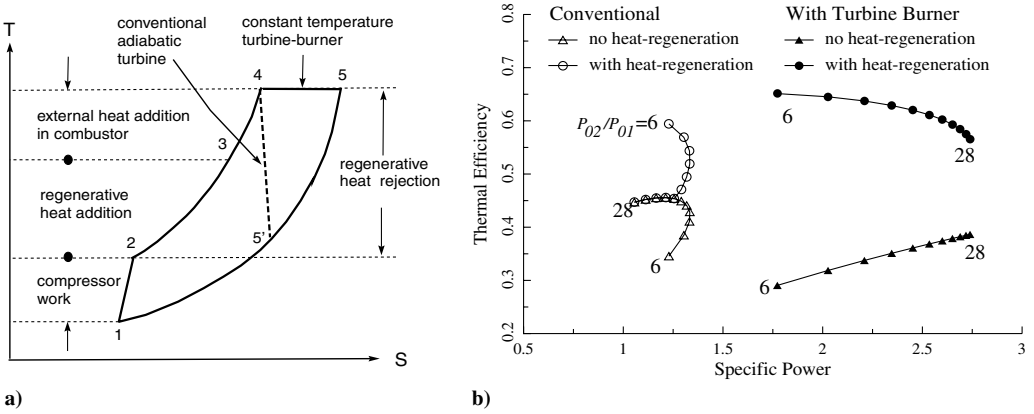

Fig. 9 Results for stationary gas-turbine engine.

power although the thermal efficiency is slightly lower than that of the conventional engine (see Fig. 9). However, with heat regeneration and the turbine burner, both specific power and thermal efficiencies are higher than in the conventional configuration with heat regeneration, but without turbine burner. A 10%–20% increase in efficiency can be achieved. The increase in specific power is particularly dramatic; a more than twofold increase in specific power can be achieved at the higher compressor pressure ratio end. Higher specific power means a smaller engine, with its various benefits, for the same power level.

Note that the cooling requirement will have a significant impact on the relative performance of the turbine-burner engines. On one hand, the use of CTBs and ITBs appears to increase the need for turbine blade cooling (for the same temperature), which reduces the benefit of the turbine-burner engines. On the other hand, one should be reminded that because of the use of the CTBs or ITBs, the combustor temperatures can be reduced to still maintain the same, or higher, thrust/power levels and thermal efficiencies. Thus, the amount of cooling may actually be reduced and, in addition, we have the added benefit of reduced NOx emission because of the lowered burner temperature. Chen et al. [3] included various cooling models in their investigation and concluded that the performance gains of the turbine burners were greatly reduced for aircraft engines, but significant gains still stood for ground-based engines. Their comparisons were made between engines using the same turbine inlet temperatures. Liew et al. [4] also studied the effect of cooling. They properly compared engines with different burner temperatures and confirmed that the turbine-burner engines indeed provided "higher specific thrust, improved thermal efficiency, less cooling air, and possibly less NOx production" when the burner temperatures are properly chosen.

III. Challenges

We have shown thermodynamically that substantial improvements in performance are theoretically possible with the turbine burner, especially at the higher compression ratios and bypass ratios projected for future designs. It remains now to realize these improvements by addressing the challenges of combustion within the turbine stage itself.

In Fig. 10, the stator and rotor passages are shown in cross section on a "rolled-out" cylindrical surface. Flow from the main combustor enters the stator passages from the left. The stator vanes turn the flow and the stator passages have a change in cross-sectional area: a convergent section to a throat followed by a divergent section. The flow is accelerated from low subsonic speeds to low supersonic speeds. The streamwise and turning accelerations can each be $10^5 g = 10^6$ m/s^2. Residence time in the stator passage can be of the order of a millisecond or less. The rotor cross section is moving along the cylindrical surface. The acceleration magnitudes and residence-time magnitudes are similar to those for the stator.

There are many challenges that face the development of a technology to allow combustion in the stator passage: ignition in a high-acceleration flow; flameholding in a high-acceleration flow; complete vaporization of liquid fuel, mixing, and combustion for a short residence time; hydrodynamic stability of a stratified flow with a large turning acceleration; increased demands for cooling of rotors and stators; and maintenance of an acceptable aerodynamic-force loading on the rotor blades. We focus our research first on the ignition and combustion issues and the hydrodynamic stability, which can affect combustion, because without successful combustion in the turbine burner, there is no need to address modifications of heat transfer and aerodynamics.

In the remainder of this paper, we first examine the literature concerning compact combustors (i.e., short residence times) and the

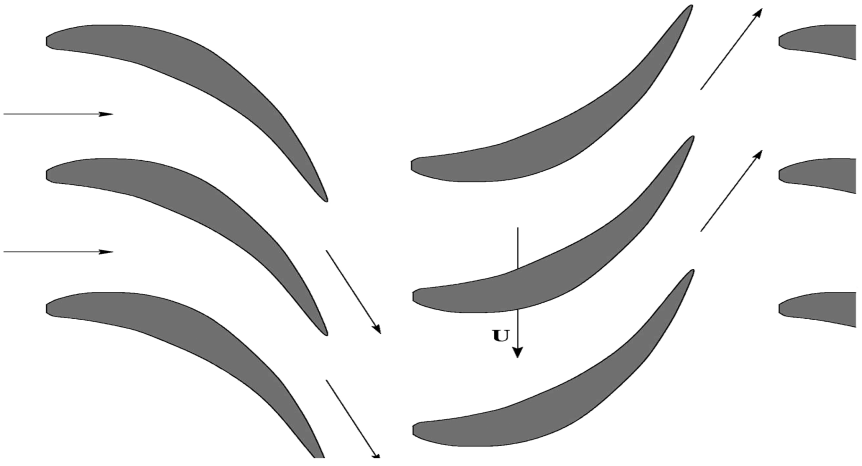

Fig. 10 Layout of stator vane and rotor blade intersections with cylindrical surface.

use of cavities for flameholding. Then we focus on combustion in accelerating flows in order to understand some fundamental issues that are critical to turbine-burner enabling technology. Classes of model problems will be treated in order of increasing complexity. We first examine the situation of mixing, ignition, and burning in a viscous shear layer (mixing layer) subjected to an accelerating pressure gradient. In the next section, we consider a free mixing layer with an imposed streamwise pressure gradient. Both laminar and turbulent cases have been examined, using the boundary-layer approximation. Then we consider mixing layers within channeled two-dimensional flows for both straight channels with axial acceleration, due to area change and curved channels with both turning and streamwise accelerations. All of these cases are in steady state; Reynolds-averaged Navier–Stokes equations are used for the turbulent flow. In the section after the next, we discuss unsteady, two-dimensional flows at Reynolds numbers in the transitional domain. The Navier–Stokes equations are used here to treat reacting mixing layers in straight channels, curved channels, converging channels, and simulated turbulent passages. In another section, we examine the use of flameholding cavities with fuel and air injection directly into the cavity that is adjacent to the flow channel. Unsteady Navier–Stokes equations are solved in both two and three dimensions.

IV. Compact Combustors and Use of Cavities for Flameholding

A. Flameholding in High-Speed Flows

There has been important research completed on the injection of liquid fuels into high-speed crossflows. This research has been motivated by the scramjet application. The U.S. Air Force Research Laboratory (AFRL) has been a leader in this area of study [5–10]. Our interest differs in the turbine-burner application, since the liquid fuel will be injected into the upstream low-speed portion of the flow where ignition and flameholding occur. The acceleration to supersonic velocities occurs over a downstream distance of about 10 cm. The challenges of injection and ignition with a high-speed flow are different from the challenges with an accelerating flow, but the spray breakup and penetration can be similar in the turbine burner to those processes in conventional burners. Shock waves will not be caused by the liquid stream as would occur in a scramjet application. The momentum ratio for gas to liquid in the region of injection, ignition, and flameholding will be significantly lower for the turbine burner than for the scramjet. Therefore, penetration of the spray should be less challenging for the turbine burner. However, the acceleration of the flow will have some important consequences. The very high acceleration ($10^5 g$) in both the streamwise and transverse directions, coupled with the flow stratification, can produce significant instabilities that would affect turbulence levels and thereby mixing times, heat transfer, ignition delay, and flame stability. Certainly, though, there are some similarities with the scramjet related to the short residence time for combustion.

Lin et al. [5] experimentally examined aerated-liquid injection into a supersonic crossflow. They demonstrated agreement with an analysis based upon previous correlations. They discovered that the sprays become denser, droplets become smaller, and penetration is larger for the aerated (effervescent) liquids. Lin et al. [6] extended that work to injection at an angle other than 90 degrees with the crossflow. They found the same qualitative conclusions. Also, they developed a model that predicts injector exit velocity and liquid-film thickness, based upon measured penetration distance.

Hsu et al. [7] measured fuel distribution resulting from a low-angle flush-wall injection upstream of a cavity and into a Mach 2 gas flow. They found that interaction of the shear layer generated on the upstream wall with the trailing edge of the cavity was an important factor controlling fuel transport into the cavity. The injection of fuel into a supersonic stream from a flush-mounted injector array was simulated [8] using a gaseous nitrogen. The above four studies [5–8] did not involve reacting flows. Combustion was considered in [9,10]. Gruber et al. [9] examined the use of a wall-cavity for flameholding. Two different injector designs, both placed on the wall upstream of the cavity were studied. Ignition and flameholding was successful over a range of equivalence ratio at combustor conditions equivalent to a flight Mach number between 4 and 5. Mathur et al. [10] were able to successfully ignite and hold a flame with jet fuel injected from a flush-wall-mounting upstream of a cavity. Spark and plasma ignition were applied at the floor of the cavity. Aeration of some of the fuel with oxygen was employed. Equivalence ratio varied between 0.9 and 1.0, and the simulated flight Mach number was between 4 and 5.

Yu et al. [11,12] have also provided some interesting results concerning the combustion of kerosene fuels in supersonic combustors. Yu et al. [11] considered kerosene injection into a Mach 2.5 crossflow of air. Pure liquid injection, aeration with air, and aeration with hydrogen were examined. The hydrogen would create a pilot flame. In some cases, hydrogen was injected separately from the kerosene. Cavities of various length-to-depth ratios were considered; sometimes two cavities in tandem were used. They found that a sufficiently small length-to-depth ratio could cause a resonance that was helpful to mixing, but not so helpful to flameholding; for that reason, two cavities in tandem with very different length-to-depth ratios were studied.

Yu et al. [11] showed that aeration is helpful and that performance increases with cavity depth (and thereby with cavity residence time). Two cavities in tandem were found to be more efficient than one; furthermore, placing the cavity with the larger length-to-depth ratio upstream of the shorter cavity provided the better performance. Combustion efficiencies as high as 92% were reported. In an earlier study [12], it was shown that the ignition delay of kerosene could be less than 1 ms if local temperature exceeded 1280 K and the mean droplet size was less than 20 μm. This provides guidance on cavity size and residence time.

Glassman [13] indicates that many common fuels (e.g., methyl alcohol, heptane, kerosene) can achieve ignition delays of 1 ms or less at temperatures of 950 to 1050°C. Hydrogen has a 1 ms ignition delay at a temperature as low as 700°C. These results are for 1 atm of pressure and ignition delays can be expected to be significantly lower at the elevated pressures of interest in jet propulsion applications. Methane is more difficult to ignite. Spadaccini and Colket [14] show that a number of investigators have been able to report methane–air ignition delays of 1 ms or less at 1254 K and 16.5 atmospheres of pressure. Note that our computational studies also indicate that ignition can occur.

One of the key elements of combustion in the systems described above is the mechanism of flameholding in high-speed flows. Although flameholding in high-speed flows has been researched extensively, most of the research is geared toward supersonic applications such as ramjet engines (see, for example, Billing [15], Abbitt et al. [16], Tishkoff et al. [17], and Ben-Yakar and Hanson [18]). The flameholding required for the turbine burner is not in such high-speed flow, but the potential methods are similar. Two approaches for stabilizing flames in flows are 1) organizing a recirculation area where the fuel and air can be mixed and 2) forming coherent structures containing unmixed fuel and air wherein a diffusion flame occurs as the gases are convected downstream. Creating a recirculation zone for mixing of fuel and air can be achieved with a step or an open cavity, which creates sudden flow expansion and hence creates a recirculation zone. The ITB and the trapped-vortex combustor described below use this technique for flame-anchoring, as do our turbine-burner studies. In all cavity flameholding situations, the amount of fuel/air naturally entering the recirculation zone from the core flow is low. Hence, fuel and air are directly injected into the cavity. Another technique for creating a recirculation zone is to have a step in the flow. Subsonic combustion stabilized by a backward-facing step has been researched [19]. The results show that the step acts as a flame anchor, and the flame blowout limits are improved, due to the presence of the curving chamber. Our experimental design takes advantage of the growing compact combustor advances and provides fundamental information regarding flameholding.

In summary, we have three bodies of scientific literature that encourage us to believe that ignition and flameholding is achievable in the high-acceleration flow of a turbine burner: the experimental

advances in supersonic combustion [5–12,15–19], the supporting ignition data [13,14], and our own computational and experimental research that includes some more difficult-to-ignite fuels (see Secs. V, VI, VII, VIII, and IX). It should be possible with the use of cavities to obtain the necessary residence times. Aeration of the liquid-fuel streams can be helpful. It might be possible to rely on autoignition, due to the hot products and air mixture flowing through the turbine burner. If not, spark ignition and pilot flames are possibilities.

B. Compact Combustors

There have been several technological approaches to reducing the overall size of gas-turbine engines by shortening the length needed for the primary combustor. The turbine burner shortens the combustor by transferring some of the heat release into the turbine vane region. The trapped-vortex combustor shortens the combustor by intensifying the reaction zone while anchoring the flame with a recirculation cavity near the fuel injector. The ultracompact combustor uses a circumferential cavity to trap the combustion zone as the reactants enter the compressor turbine stages. The ITB is a related concept in which some of the combustion is expected to take place between turbine stages, thereby shortening the needed primary combustor. A final concept has been termed in situ combustion, where fuel is injected directly into the turbine vane region. Although not identical to the combustion challenge posed by the curving contracting flows in the turbine burner proposed, these concepts are related to the research proposed in that many of them involve fuel injection, mixing, and flameholding in high-speed flows. They are each discussed further below.

1. *Trapped-Vortex Combustor*

The trapped-vortex combustor (TVC) concept is the result of fundamental studies on flame stabilization performed by researchers at the AFRL and GE Aircraft Engines under the joint sponsorship of AFRL, the U.S. Navy, and the Strategic Environmental Research Development Program [20], during the last 10 years, and it is still under investigation. This new kind of combustor is connected to our research in that it addresses the problem of flame stabilization and flameholding inside the combustor through the use of small cavities. Instead of swirl stabilized combustion, the trapped-vortex combustor maintains flame stability with a vortex trapped in a cavity inside the combustor. The vortex is protected from the main flow inside the combustor and acts as a pilot flame and provides a continuous ignition source for the main combustor. In a TVC, strategically-placed air and fuel injection points in the forward and rear walls of the cavity drive the vortex in the cavities. The part of fuel injected into the cavities mixes and burns quickly in the stable trapped-vortex flow structure. The created vortex recirculates the hot combustion gases within the cavity. The cavity recirculation driven by the injection is also important in our turbine-burner channel flows. Initial studies with the TVC have shown substantial combustion improvements over traditional combustors. For example, a TVC used in a rich-burn, quick-quench, lean-burn system may reduce NO_x in ground-power gas-turbine engines that operate on low-cost fuels containing fuel-bound nitrogen [20,21].

A numerical evaluation of the TVC is also underway [22]. The configuration is formed by a forebody and afterbody of opportune depth and separation distance. Main air flowing over the cavity forms a recirculation region within the cavity. Fuel and air are injected into the cavity through the afterbody face in a way that reinforces the primary vortex direction of the recirculating flow. At Georgia Tech, additional computational investigations about the TVC have been performed [23].

Ramjen Power Systems, Inc., is attempting to commercialize a lean-premixed trapped-vortex combustor [24]. This TVC is fired on methane. Their TVC prototype relies on locking a vortex structure between the fore and aft bodies of the cavity. Interaction between the highly turbulent, hot cavity gas and the cold channel flow is promoted using flame stabilizing features placed in the channel flow. Recently, a combined computational and experimental study of single cavity trapped-vortex combustion has demonstrated low-pressure drop generated by the cavity and dynamic links between the combustion processes and cavity dimensions [25,26].

The above trapped-vortex combustor studies provide a useful guide to the design and building of our own combustion apparatus, because they relate cavity size and chamber size to obtain efficient, stable, and clean combustion. In particular, the examples showed that high-accelerating flow ducts based on cavity flow stabilization can be built at sizes that can fit inside the space of a turbine stage. They also show how fuel and air injection can either support or disrupt a cavity recirculation.

2. *Ultracompact Combustor*

One version of a more aggressive TVC is being called the ultracompact combustor (UCC). Studies on the UCC are underway at the AFRL [27–29]. This type of combustor incorporates several of the principles of the turbine burner. The UCC concept combines the combustor with the compressor exit guide vanes and the turbine inlet guide vanes. In a conventional annular combustor, air enters the combustion chamber through dome swirlers and liner holes that provide mixing air and cooling air to the system. In the UCC concept, a cavity runs around the outer circumference of the extended turbine inlet guide vanes [29]. All of the fuel is introduced into this cavity. Aligned with this cavity, on each vane, there will be a radial cavity that extends to the inner platform. The idea is to burn rich in the circumferential cavity, allowing much of the required combustion residence time to take place in the circumferential direction of the engine, rather than in the axial direction as is done conventionally.

Flame stabilization occurs as combustion products recirculate in the cavity. The intermediate products of combustion are transported by lower wake pressures into the radial cavities in the vane surfaces where combustion continues at a reduced equivalence ratio as the mainstream air is entrained into the wakes. Finally, across the leading edge of the vanes, again in a circumferential orientation, there is a minimum blockage flameholder (strut) where products are entrained and distributed into the main flow. Practically, the circumferential cavity may be regarded as a primary zone, the radial cavities as constituting an intermediate zone, and the circumferential strut flameholder as the dilution zone. In some contrast to the turbine-burner approach, all combustion is intended to be completed before any flow-turning and acceleration caused by the turbine inlet guide vanes. The cavities can be seen as a folded combustion system so that the rich-burn, quick-quench, lean-burn process actually starts at the inlet of the combustor with the rich-burn process taking place in parallel in the cavities and is accomplished without extending the length of the combustion system.

The UCC rig realized at the AFRL simulates turbine inlet guide vanes, and an experimental investigation of a high g-loaded combustion system has been successfully conducted in an atmospheric pressure rig [28]. The results indicate that this type of combustion system has the potential to be used as an ultracompact combustor for a main burner, or as an ITB for use as a reheat cycle engine.

The main results of the tests on the UCC revealed the following:

1) High combustion efficiencies over a wide operating range.

2) Short combustion lengths compared with conventional combustion systems operating at similar conditions.

3) Higher heat release rate compared with conventional combustor designs by a factor of 2.

4) Stable, efficient operation at 2–3-times-higher combustor loading than for conventional systems.

5) Excellent lean-blowout performance.

6) The radial-vane cavity effectively transports the mixture from the cavity to the main airflow.

7) The unreacted mixture transport into the main airflow is a strong function of injector air and cavity g-loading. Increased g-loads create a centrifugal effect in the cavity, keeping the unreacted mixture toward the cavity outside diameter. However, a limit is reached where

flame extinction occurs in the cavity, due to high velocities that are unable to sustain the flame. Therefore, a window of optimal g-loading seems to be 500–3500 g.

8) Pressure effects improve the combustion efficiency for a given configuration, but have little impact on the lean-blowout performance.

The experiments on the UCC are important for turbine-burner research in that they provide useful information about combustion in high accelerating flows and flameholding within small cavities connected to the main duct. One of the differences between the UCC and the kind of system we employ is that rather than a simple cavity, the UCC involves two types of cavities working at the same time, the circumferential cavity and the radial-vane cavity.

A further development of the UCC concept is represented by the cavity-inside-cavity (CIC) design [30]. The main idea of this type of burner is to add a second cavity, channeled inside the primary one. All of the fuel used in the UCC is injected through the secondary cavity. Additional air jets are also used in the CIC for increasing fuel/air mixing and for creating a vortical flow inside the cavity. For an earlier history of UCC work, see [31–33].

3. *Interturbine Burner*

Another related approach is the ITB, where combustion occurs between the high- and low-pressure turbine to act as an internal reheat stage. The U.S. Department of Defense made a Small Business Innovation Research call for demonstrating ITB technology for improving part-power performance of turbine engines. The call cited some preliminary studies indicating that the part-power fuel efficiency can improve by 7 to 17% by using an ITB. Three companies received Phase I support to pursue the ITB. Creare, Inc., examined potential benefit using cycle analyses. Spytek Aerospace Corporation attempted to add an ITB to an existing engine with particular attention to providing air into the primary burn zone of the ITB and to successfully entraining the combustion products into the main stream flow. Advanced Products Research, Inc., had prior experience with trapped-vortex combustors and planned to work with Honeywell Aircraft Engines to detail ITB designs and their integration into small gas-turbine engines. Because of their commercial nature, these studies have not yet been fully documented, but they demonstrate the growing feasibility of employing novel integrated combustor-turbine designs to take advantage of more compact engines and the use of internal reheat stages.

4. *In Situ Combustor*

Siemens Westinghouse Power Corporation is developing a so-called in situ reheat combustor (fuel injection via airfoil injection) as a means for increasing cycle efficiency and power output, with possibly reduced emissions [34]. This kind of device has an application very similar to the one of the turbine burner. The objective of the Siemens project is to develop a gas reheat concept for gas-turbine engines, in which fuel is injected directly into the turbine through one or more stages of vanes and blades. The base concept is to add enough fuel at the vane trailing edge to restore the working gas temperature to the turbine inlet temperature. Numerical simulations were set up to estimate the performance of the in situ reheat cycles at turbine offdesign conditions.

The in situ reheat process model is another idea under investigation. It is basically identical to the sequential combustion reheat, but the reheat combustor basket used with sequential combustion reheat is replaced by an in situ combustor representing the flowpath between vane and blade. With in situ reheat, sufficient fuel gas is injected through the high-pressure turbine-stage airfoils, rather than through reheat combustor baskets, with reheat-combustion proceeding in the wakes of the airfoils. The ability to complete combustion between the high-pressure stage and the low-pressure turbine, while avoiding overheating of the airfoils, has not yet been demonstrated. The turbine-burner concept can be viewed partly as a reheat strategy, but one that is fully integrated into the flow configuration.

V. Reacting Free Mixing Layer in Accelerating Flows

Combustion in the turbine-burner passages will involve turning and streamwise acceleration of the flow through the transonic range. There is a lack of fundamental treatment in the literature of multidimensional flows with mixing and chemical reaction in the presence of strong pressure gradients that support a transonic flow. For zero-pressure-gradient conditions, many investigators have considered reacting, multidimensional (laminar and turbulent) low-Mach-number mixing/boundary-layer flows using a wide variety of approaches. See, for example, Marble and Adamson [35], Emmons [36], Chung [37], and Sharma and Sirignano [38] for laminar flows, and see Patankar and Spalding [39], and Givi et al. [40] for turbulent flows. A limited number of efforts have been made on reacting supersonic flows (see, for example, Buckmaster et al. [41], Grosch and Jackson [42], Jackson and Hussaini [43], Im et al. [44,45] and Chakraborty et al. [46]). For a two-dimensional, laminar, nonreacting boundary layer over a solid body with a pressure gradient, similarity solutions were obtained by Li and Nagamatsu [47], Cohen [48], and Cohen and Reshotko [49] solving the momentum and energy equations transformed by the Illingworth–Stewartson transformation [50–52].

Our research on laminar, reacting, accelerating mixing-layer flows resulted in two studies. Infinite chemical-kinetic rate and a reaction zone of zero thickness were assumed by Sirignano and Kim [53], who reduced the partial differential equations to a system of ordinary differential equations and obtained similarity solutions for laminar, two-dimensional, mixing, reacting and nonreacting layers with a pressure gradient that accelerates the flow in the direction of the primary stream (see Fig. 11). By constraining the relationship between the two freestream velocities, a similar solution for the two-dimensional, steady flow may be found. These similarity solutions, shown for temperature in Fig. 12, offer some insight into the effect of flow acceleration on the flame structure in the mixing layer. However, they are only valid for restricted classes of flows with particular pressure gradients. Moreover, they cannot predict the ignition process close to the trailing edge of the splitter plate. The similar solution with the infinite-kinetics-rate assumption, only applies to the fully established diffusion-controlled downstream flame region. Because of variable density and speed of sound, the flow can change between subsonic and supersonic domains in the transverse direction.

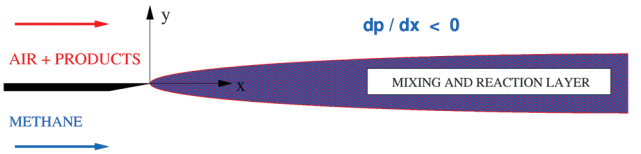

Fig. 11 Sketch of reacting mixing layer subject to pressure gradient.

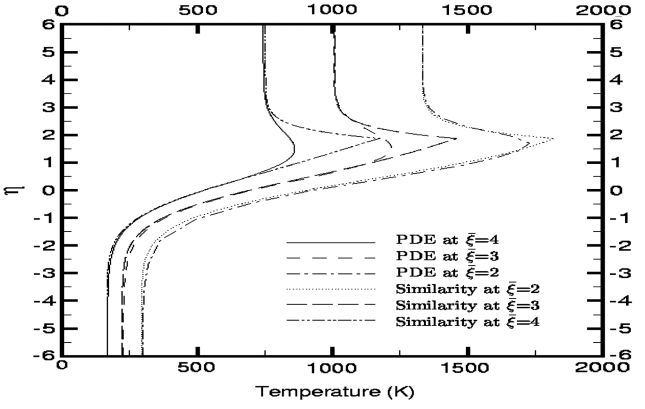

Fig. 12 Mixing-layer temperatures for reacting, accelerating mixing layer [53,54].

In the second study on laminar mixing layers [54], finite one-step chemical-kinetic rates were considered, and nonsimilar solutions were obtained by numerical integration of the steady-state 2-D partial–differential equations obtained through the boundary-layer approximation. So both the ignition process and the established flame were examined. While the analysis was motivated by applications to the gas-turbine engine, the approach was to address an idealized problem that had the critical features of mixing and chemical oxidation in a gaseous flow that is accelerating through the transonic range. A mixing layer was considered, rather than a channeled elliptic flowfield, in order to simplify the calculations. Similarly, one-step chemical kinetics was taken even though some error occurs when the same scheme is used for both ignition and the established flame. Methane was taken as the fuel, since its properties are well documented, and it does have application for some ground-based gas-turbine engines. Laminar flow was considered. In the first problem considered, these gross simplifications can still produce some useful results and insights; some salient characteristics of the flow can be identified with this simplified model.

Methane gas flowed on one side of the mixing layer with heated air or vitiated air on the other side. So the chemical balance is described by

$$CH_4 + 2O_2 + 7.52N_2 \rightarrow CO_2 + 2H_2O + 7.52N_2 \qquad (1)$$

The chemical-kinetic rate is given as a one-step mechanism:

$$\omega_F = -A\rho^{(a+b)} Y_F^a Y_O^b e^{-E/RT} \qquad (2)$$

where Y, T, and ρ represent mass fraction, temperature, and density; E, A, a, and b are constants; and subscripts O and F denote oxygen and fuel.

For laminar flows, the mixing layer remains very thin. For the accelerating flow, the peak temperature is found to decrease with downstream distance. This implies that NO_x formation would be less than that which occurs in a flow without acceleration. A mixing and exothermic chemical reaction in the accelerating flow through the turbine passage therefore offers an opportunity for a major technological improvement. The reduction in peak temperatures due to acceleration results in the promise of reduced pollutant formation and reduced heat transfer losses in many other combustion applications.

A wide range of accelerations, initial pressures, and temperatures were considered. Sensitivities to transport properties and kinetic parameters were determined. Ignition delays were affected substantially by some of the parameters. Comparisons with the similar solution [53,54] are made in Fig. 12; it is shown that agreement is good except for the reaction zone. Obviously, the maximum temperature occurs in the reaction zone that has zero thickness for the similarity solution causing a cusped profile.

The region of higher temperature will have a reduced gas density. Consequently, for the given pressure gradient, the low density, high temperature will accelerate more than the surrounding gas, producing a velocity overshoot, as indicated in Fig. 13. However, the high-temperature region also has a higher speed of sound. Therefore, in spite of its higher velocity, it can have a lower Mach number than the surrounding gas. This result is indicated in the Mach number contour plot of Fig. 14. In fact, the reaction zone can have a subsonic flow while the surrounding gas is supersonic. The importance of pressure gradient and initial pressure is shown in Fig. 15. A finite difference method was developed [54] for solving the two-dimensional mixing-layer equations with chemical reaction without the use of the similarity assumption. We first compared computational results with the similarity solutions [53] and then extended our computations to nonsimilar cases in order to examine the ignition and combustion processes in a general accelerating mixing layer.

Streamwise transport rates were found to be much smaller than lateral transport rates thereby justifying the use of the boundary-layer approximation for the mixing layer.

Reference [55] extends the works of [53,54] by considering a two-equation model of turbulence for the accelerating, transonic, reacting

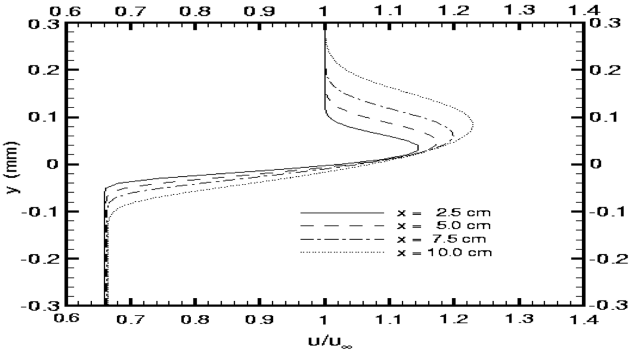

Fig. 13 Streamwise velocity profile for reacting, accelerating mixing layer [54].

mixing-layer mean flow with gaseous fuels. The boundary-layer approximation is maintained in this work. The ignition delay, mixing-layer thickness, flame temperatures, and velocity profiles are determined for a wide parameter range, including pressure gradient magnitudes and upstream velocities. Ignition delays and locations and standoff of the established flame zones were predicted. Temperature and oxygen contours are shown in Fig. 16.

A premixed region occurs near the leading edge of the flame as oxygen diffuses across to the fuel side. Some distance from the trailing edge of the splitter plate is required before ignition occurs

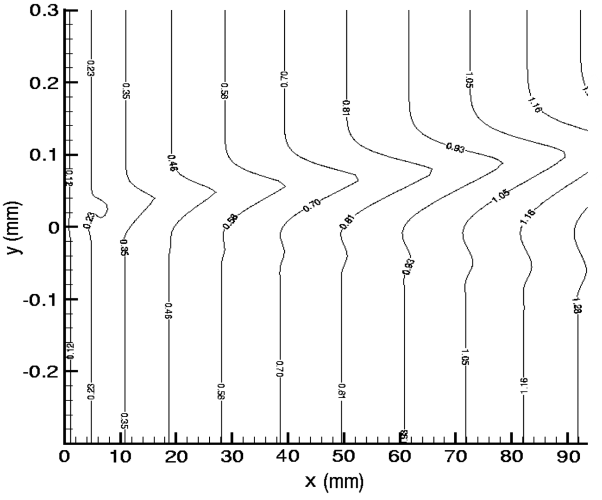

Fig. 14 Mach number contours for reacting, accelerating mixing layer [54].

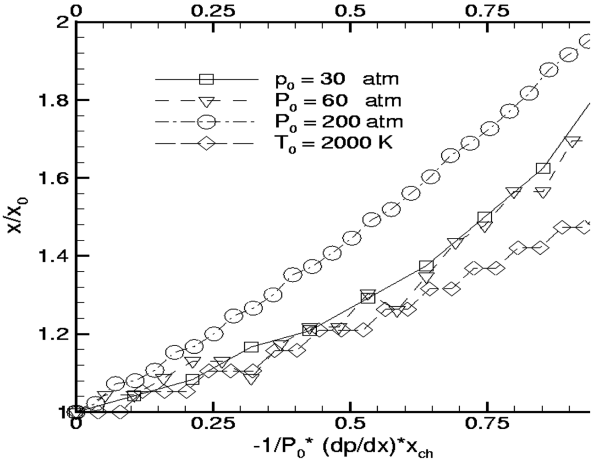

Fig. 15 Effects of pressure gradient and initial pressure on ignition delay [54].

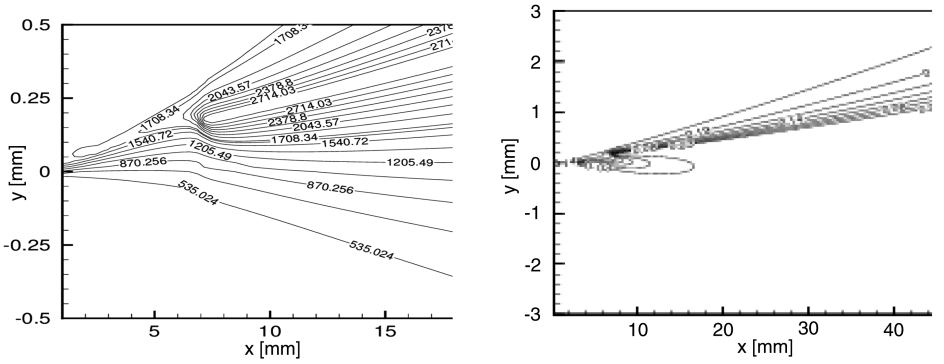

Fig. 16 Turbulent mixing layer: a) temperature and b) oxygen contours.

(ignition delay) and a flame is established. The turbulent boundary-layer thickness grows faster downstream than does the laminar thickness. Qualitative similarities do exist between the laminar and turbulent cases with regard to temperature, mass fractions, velocity, and Mach number profiles.

VI. Reacting, Accelerating, Turbulent Channel Flows with Mixing Layer

A key to the turbine burner is the mutual interaction between the combustion processes and the flow through the turbine blade rows. Although there has been much work on computation of reactive flows, there is none on high-acceleration reactive flows in turbomachines. We therefore examine reacting flows that are accelerated through channels and passages. We continue with mixing-layer configurations first.

Turbulent reacting methane–air mixing-layer flows in ducted channels have been modeled by both a Baldwin–Lomax algebraic model [56] and a two-equation k-ω model [57]. The flow variables are averaged across the spanwise direction, with a varying span along the flow direction that results in the cross-sectional area change that produces the streamwise pressure gradient. Here, the boundary-layer approximation was no longer made. That is, fully elliptic, quasi-two-dimensional, Reynolds-averaged Navier–Stokes equations are considered. The fuel is injected at the upstream end of the channel between two airstreams. So diffusion flames are established on both sides of the fuel stream. Also, turning channels were considered. This introduces a transverse acceleration as well as the streamwise acceleration. Various turbulent results indicate that ignition can occur and a flame can be held in these high-acceleration turbulent turning or straight-channel flows.

The boundary-layer approximation was used in parallel computations for the same configurations, and the results compared well with the elliptic calculations. Two curved channels with different curvature radii were compared with the straight channel. Transverse accelerations up to 10^5 g were examined. Flames were maintained in all cases, but velocity and scalar profiles varied significantly.

VII. Reacting, Accelerating, Transitional Channel Flows with Mixing Layer

Computational analysis by Cheng et al. [58–60] has addressed transitional accelerating (and nonaccelerating) and reacting (and nonreacting) flows using direct numerical simulation of the Navier–Stokes equations and allowing time-dependent computation. Again, the flow variables are averaged across the spanwise direction with a varying span along the flow direction that results in the streamwise pressure gradient. Gaseous methane fuel flows parallel to air at the inlet. The unsteady mixing layer has been analyzed without the boundary-layer approximation so that upstream influence may occur. The instability of the mixing layer and its effect on mixing rates has been demonstrated. The conclusion is that the flow through the simulated vane passage is unlikely to be close to fully developed turbulence. So Reynolds-averaged and Favre-averaged approaches should be abandoned. Rather, direct numerical simulation and, where necessary because of resolution issues, large-eddy simulations should be used.

For these studies, Cheng et al. [58–60] developed a finite difference numerical method for compressible, multicomponent, reacting flows for a generalized coordinate system. The two-dimensional coordinates x and y are transformed into generalized coordinates ξ and η, which need not be orthogonal to each other. This transformation is used for ease of treating curved walls and nonuniform meshes. The inviscid flux is discretized using a flux-splitting algorithm with a second-order upwind total-variation-diminishing scheme to suppress overshoots. Second-order central differencing is used for the viscous flux, and a second-order Runge–Kutta multistage scheme is used for time-marching. The code is capable of capturing shock waves. It has been validated using comparison with exact solutions in specific test cases and with certain experimental data on unsteady mixing layers [58].

The Cheng et al. study has given attention to the effects of various instability types: Kelvin–Helmholtz (KH), Rayleigh–Taylor (RT), and centrifugal. The KH instability results from the injection of a fuel stream into the hot oxidizing gas with a relative velocity, while the RT results in turning flow, due to the different densities of the fuel stream, the oxidizing stream, and the product stream. The centrifugal instability can result at specific angular-momentum distributions. Rayleigh, as reported in [61], showed that a necessary and sufficient condition for stability with axisymmetric disturbances to a two-dimensional, inviscid, uniform-density, curved flow is that the square of the angular momentum (product of velocity and streamline radius of curvature) does not increase with radial position. So if our curved channel has a faster stream on the outer side of the curve, this would be destabilizing, due to the centrifugal instability. If the outer stream is hot and less dense, as well as faster, we can have both RT and centrifugal instability, in addition to, of course, the Kelvin–Helmholtz instability. Although it is a three-dimensional phenomenon in the pure form, the angular-momentum criterion can modify the KH instability in two dimensions.

Computations have been performed for reacting mixing layers with turning acceleration [59] and with both turning and streamwise acceleration [60]. Figures 17a and 18 show temperature contours for calculations with hot air flowing on the outside of the curve while cold methane gas flows on the inside. Figure 17b shows the vorticity contours. In those cases, there is hot, oxidizing gas flows on the outer side of the mixing layer with cold-hydrocarbon gaseous fuel on the inner side. In this case, we expect some Rayleigh–Taylor instability, due to the density gradient, as well as Kelvin–Helmholtz instability. Centrifugal instability can also occur, which is not dependent on density variation, but rather on streamwise velocity variation in the transverse direction.

Computational studies [60] have also been performed on nonpremixed flows in accelerating and turning channels that simulate the turbine stator passage. A mixing-layer flows into the simulated stator passage; hot oxidizing gas flows on one side of the mixing layer with cold-hydrocarbon gaseous fuel on the other side.

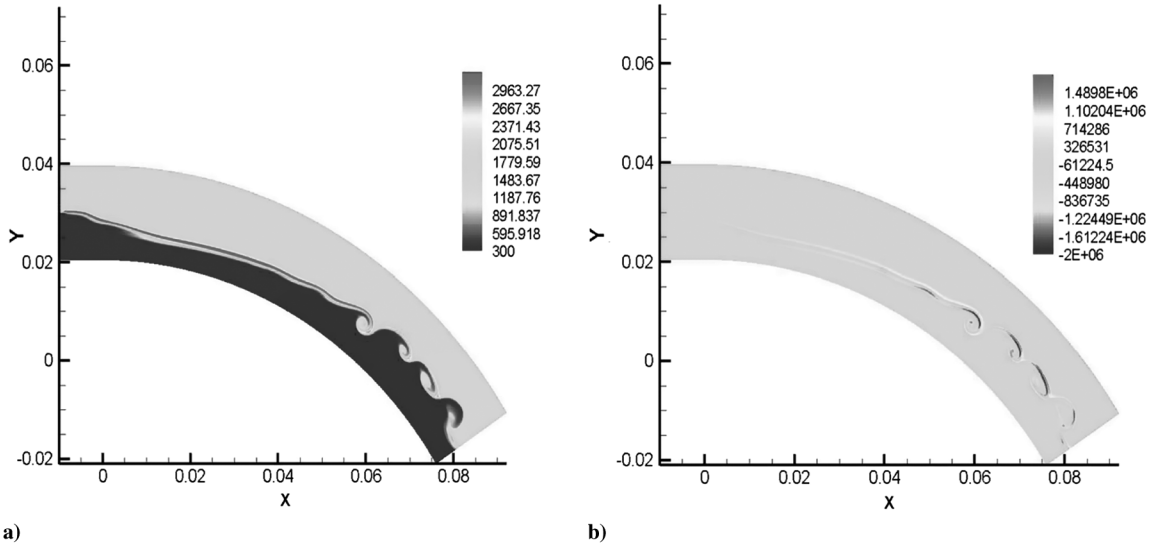

Fig. 17 Mixing-layer flow in curved channels: a) temperature and b) vorticity [59].

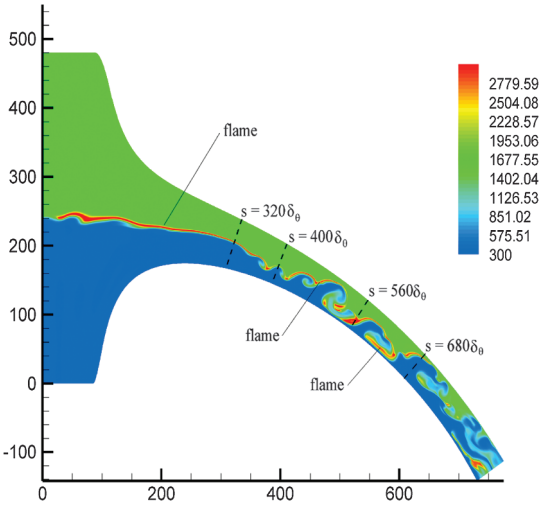

Fig. 18 Instantaneous temperature for reacting mixing layer in curved, converging channel.

Cavities have not yet been used in those two-dimensional, unsteady flows where the fluid accelerates from low subsonic speeds to low supersonic speeds, undergoing transition to turbulence. These computations have shown that the reacting flow in the passage results in greater turbulent kinetic energy and mixing, as compared with the nonreacting case. Figure 19 shows a calculation in a channel shape that represents an actual stator passage, including space between the stator and rotor. The same type of behavior as seen in the converging–diverging channel occurs. So this finding gives evidence of the value and relevance of the experimental studies that will be discussed later.

Cheng et al. [58–60] have shown that the reacting flow in the passage results in greater turbulent kinetic energy and mixing, as compared with the nonreacting case. Our explanation in the mixing-layer velocity and density profiles for the reacting case is that there will be a minimum of density value and a maximum of velocity value, which increases the number of inflection points and intensifies the instability. The KH instability is the major effect, while the RT and centrifugal instabilities can add or subtract to the effect of the KH instability, depending on whether the flow on the outside of the curved channel contains the faster or slower and more dense or less dense stream. (The "outside" of the curved-channel flow means the flow adjacent to the simulated pressure side of the stator vane, while the "inside" of the curved-channel flow means the flow adjacent to the simulated suction side of the stator vane.)

Centrifugal acceleration is an important phenomenon in the high-g flow through a turbine burner. Limited research has been performed on the centrifugal effect on combustion. The computational analyses [56,57,59,60] considered turning flows with high centrifugal accelerations, as discussed above. A large experimental effort at the U.S. Air Force Research Laboratory [29,62–64] has existed for research on the ignition, flameholding, and combustion of sprays in flows with high centrifugal acceleration. Our experimental work for gaseous or liquid fuels on reacting flows with high streamwise and turning accelerations will be discussed below, where we review more recent work.

VIII. Recent Computational Research on Turbine-Burner Configuration

The University of California, Irvine (UCI) program addresses the two-way coupling between combustion processes and fluid dynamical phenomena associated with burning liquid fuels in high-speed, accelerating and turning turbulent flows of the type projected for turbine burners. There is a need to understand the effects of high accelerations in the stratified flow on the turbulent mixing and flameholding, with emphasis on the role of a wall cavity. Experiments and computations have improved the scientific understanding of the effects of wall contours on the combustion. Flameholding and the amount of fuel burned can be varied by considering several fuel and air injection strategies with different

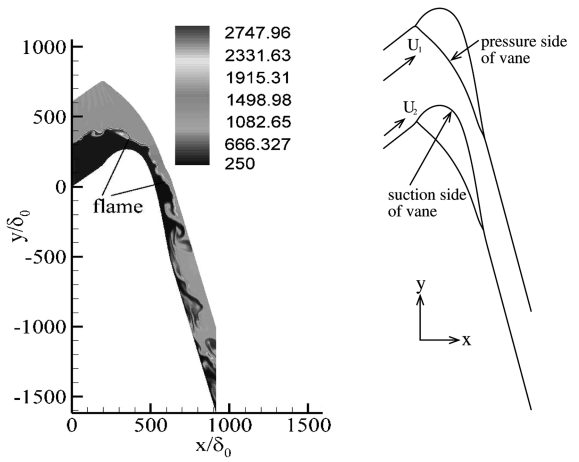

Fig. 19 Temperature contours for reacting, accelerating, transonic mixing layer in simulated turbine passage.

cavity dimensions and locations. The Reynolds numbers of interest are in the transitional range.

Computations have been performed for reacting and nonreacting flows in channels with and without cross-sectional-area change, adjacent cavity, and centerline curvature. So evaluation has been made of the effects of streamwise acceleration, turning flow, and a cavity on mixing and of the effect of fuel injection into the cavity on mixing and flameholding. Experiments have been performed for reacting and nonreacting accelerating channel flows with an adjacent cavity. Both gaseous and liquid fuels have been injected into the cavity.

A. Two-Dimensional Nonreacting Flow Past a Cavity

Calculations were first performed for nonreacting flow over a cavity in a straight channel. The flow here is incompressible and isothermal. The boundary conditions are constant, uniform inlet velocity; no slip at all of the walls; constant, uniform pressure at the exit; and a Lagrangian derivative of velocity is zero normal to the exit.

For flow over a cavity, Rossiter [65] has described a feedback mechanism between the flowfield and the acoustic field and derived a semi-empirical formula for the frequencies of the periodic vortex shedding at the cavity leading edge:

$$St_n = \frac{fL}{U} = \frac{n - C}{\xi + 1/\kappa} \tag{3}$$

$$\xi = \frac{M}{\sqrt{1 + \frac{\gamma-1}{2}M^2}} \tag{4}$$

where St is the Strouhal number, n is the mode number of oscillation, f the frequency, L the cavity length and U the freestream velocity. C is a correction factor, M is the Mach number, and κ is the ratio of the convective velocity of the vortices to the freestream velocity. This feedback mechanism is referred to as a shear-layer mode mechanism. For cavities with higher length-to-depth ratios L/D, a different mode of oscillation, known as the wake mode, was observed by Gharib and Roshko [66]. Figure 20 shows a Rossiter mode, which is found for cold flow in deep cavities without injection. These periodic modes have not been seen for shallow cavities, cavities with injection, or reacting flows.

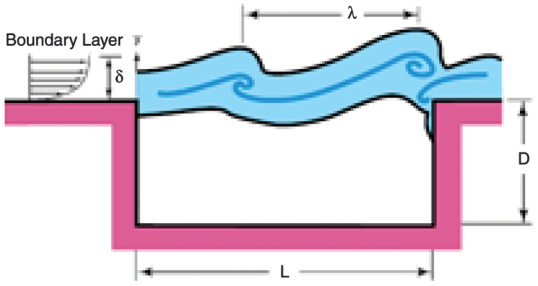

Fig. 20 Rossiter modes.

Colcord and Sirignano [67] have considered low-Mach-number two-dimensional, unsteady flow over cavities. For cavity L/D ranging from 1 to 2 and in the Reynolds number range from 5000–40,000, the results have shown Strouhal numbers that closely match Rossiter's formula for n equal to either 1, 2, or 3. It remains unclear which mode number will be selected for a given configuration. For cavities with L/D of 4, a wake mode is observed for Reynolds numbers from 5000–10,000. It is also observed that the vortex interaction inside the cavity and the influence on the main channel flow increases with L/D, as shown in Fig. 21. Square-cavity results agree with the experimental results of Sarzi-Amade [68].

Colcord and Sirignano [69] considered gaseous injection into a cavity at a steady rate. Unsteadiness is found to occur at Reynolds numbers as low as 950. The Strouhal number is shown to be close to a constant value of 2.0 for Reynolds numbers from 5000 to 10,000 and cavity (length/depth) aspect ratios of $L/D = 1.0$ and 2.0. It appears that the injection disrupts Rossiter's feedback mechanism and the oscillation frequency is instead determined by the interaction between the jet and shear-layer instabilities. Rossiter's formula no longer applies. In 3-D computations, the round jet flowing into the cavity might be less disruptive than our 2-D jet, however. Also, liquid injection should have some different consequences from those of gaseous injection.

For a cavity with a length-to-depth ratio of 2, the flow is found to be steady at $Re = 2000$ and unsteady at $Re = 3000$. Results without injection at higher, unsteady, Reynolds numbers for different cavity sizes are summarized in Table 1. The length L and depth D of the cavity are normalized by the height of the channel, and the Reynolds number is based on the channel inlet height and velocity. The Strouhal number is calculated from the dominant observed shedding frequency, which correlates to the n-th Rossiter mode. For the cases with $L = 2$, $D = 0.5$, wake modes were observed and Rossiter's formula does not apply.

Significant differences between the shear-layer mode and the wake mode can be seen in the vorticity contours of Figs. 21a and 21b. The inlet Reynolds numbers are the same for these two cases. Figure 21a shows a case with a square cavity of $L/D = 1$. A single large vortex fills the cavity and the vorticity in the shear layer is confined to the boundary layer downstream of the trailing edge of the cavity. With $L/D = 4$, a wake mode develops, as shown in Fig. 21b. Here, a large vortex can be seen forming near the leading edge of the cavity, while an ejected vortex can be seen downstream of the cavity. This vortex is ejected far enough into the channel to affect the boundary layer on the top wall. These nonreacting flows without injection indicate that the aspect ratio of the cavity will have a significant impact on the fuel/air mixing in the cavity. A cavity with a higher aspect ratio is expected to promote mixing better than a deep cavity.

When air is injected steadily into the cavity from the upstream wall, unsteadiness is found to occur at $Re \cong 950$. Without injection, the flow is steady at $Re = 2000$. The mass flow of fluid injected into the cavity is 10% of the mass flow in the main channel. Simulations of the same injection flow rate into a quiescent field show that the jet alone is steady, implying that there is a coupling between the channel flow and the injection that causes transition to unsteady behavior to occur at lower Re. With the mass ratio fixed at 10%, the Strouhal

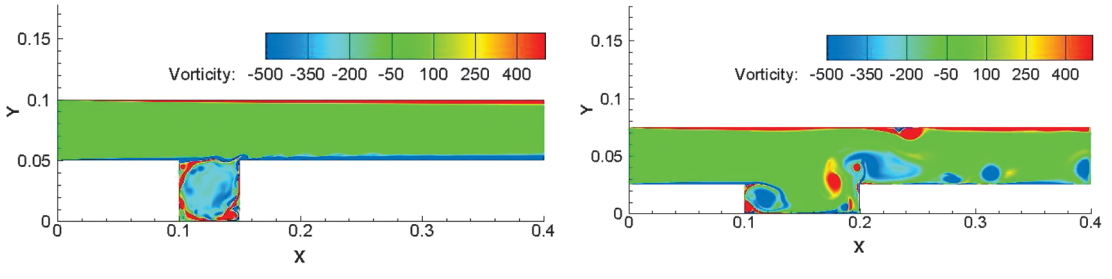

a) b)

Fig. 21 Vorticity contours at $Re = 10,000$ for a) $L/D = 1$ and b) $L/D = 4$.

Table 1 Nonreacting flow over cavity

Cavity length L	Depth D	Reynolds number Re	Strouhal number St	Rossiter number n
1	0.5	10,000	0.51	1
1	1	10,000	1.47	3
1	1	20,000	1.68	3
1	1	40,000	0.58	1
1.5	1	10,000	1.05	2
1.5	1	20,000	0.48	1
2	1	10,000	0.57	1
2	1	20,000	0.73	2
2	0.5	5,000	0.28	Wake mode
2	0.5	10,000	0.25	Wake mode

number is shown to be close to a constant value of 2.0 for $Re = 5000$–$10,000$ and for two aspect ratios of $L/D = 1.0$ and 2.0.

B. Two-Dimensional Reacting Flow Past a Cavity

Colcord and Sirignano [67] also examined two-dimensional, low-Reynolds-number reacting results ($Re < 2000$) with gaseous heptane injected into the cavity. This study has shown that the flame becomes unstable at $Re \approx 2000$ with gaseous heptane fuel injected at stoichiometric proportions from the upstream wall of the cavity. The unsteadiness increases the mixing and the amount of fuel burned. The calculations showed that for low Reynolds numbers, a single diffusion flame is present, anchored in the shear layer crossing the cavity. After a sufficient time, all of the oxidizer in the cavity beneath the flame is consumed, limiting the amount of fuel burned. With this configuration, injecting additional air into the cavity creates a secondary flame and has a significant effect on the burning efficiency. The location of the injection point also affects the burning efficiency, with injection from the upstream cavity wall providing the highest combustion efficiency of those considered.

A new compressible-flow code was employed for the reacting-flow studies while an incompressible code had been used for the nonreacting studies of the previous subsection. The combustion of gaseous n-heptane is described by a one-step overall chemical reaction: $C_7H_{16} + 11(O_2 + 3.76N_2) \rightarrow 7CO_2 + 8H2O + 41.36N_2$. The chemical kinetics rate for the fuel is estimated by Eq. (2) with the chemical rate constants $A = 1.2 \times 10^9$, $a = 0.25$, $b = 1.5$, and $E_a = 1.255 \times 10^8$, which have been obtained from Westbrook and Dryer [70].

Gaseous heptane is injected into the cavity at an overall equivalence ratio of 1.0 with the air flowing into the main channel. The air inflow and fuel injection temperatures are 1000 K and 300 K, respectively. For longer cavities and lower Reynolds numbers, the air temperature is sufficiently high for spontaneous ignition without any additional heat source. Otherwise, an added igniter is required. The walls of the channel and cavity are isothermal, fixed at 600 K. At an inlet Reynolds number of 1000, and with fuel injected from the center of the upstream wall of a cavity with $L/D = 2$, as shown in Fig. 22, 32% of the injected fuel is burned before exiting the channel. This is a slight increase over the burning efficiency of 28% achieved by injecting directly into a channel without a cavity. In the case with the cavity, the flow above the flame and the flame itself are steady. Some unsteadiness still occurs inside the cavity and in the boundary layer beneath the flame.

A burning efficiency is defined globally based on an energy balance:

$$\eta_c = \int_{t_0}^{t_0+T} \int \dot{\omega}_F \, dV \, dt \Big/ \int_{t_0}^{t_0+T} \dot{m}_{F,i} \, dt \tag{5}$$

The mixedness parameter is defined locally as

$$M = 1 + \frac{(y_C - y_{C,m})(y_N - y_{N,m})}{m^2} \tag{6}$$

where y_i is a modified mass fraction:

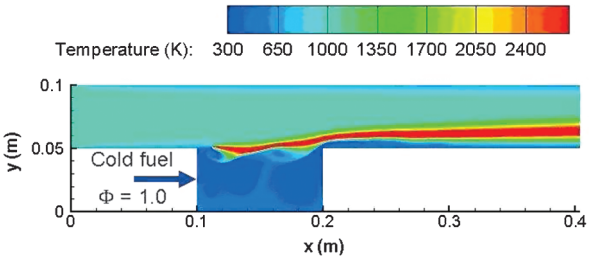

Fig. 22 Fuel injection from the upstream wall at $Re = 1000$.

$$y_i = \frac{Y_i}{Y_C + Y_N} \tag{7}$$

Note that Y_C is the mass fraction of carbon atoms, Y_N is the fraction of nitrogen atoms, and $y_C + y_N = 1$. Furthermore, $y_{i,m}$ is the perfectly mixed modified mass fraction of element i, and m is used to enforce a mixedness of zero if completely unmixed for either Y_N or Y_C approaching zero. In particular,

$$m = \begin{cases} y_{C,m}, & Y_C < Y_{C,m} \\ y_{N,m}, & Y_C > Y_{C,m} \end{cases} \tag{8}$$

For the same cavity size and injection configuration, but with $Re = 500$, the burning efficiency increases to 34%, due to the increased residence time in the channel. Burning efficiency also increases when the Reynolds number is increased to 2000, despite a decrease in the residence time. This is because the downstream portion of the flame has become unsteady, as shown in Fig. 23, resulting in greater mixing. In this case, 61% of the fuel is burned before leaving the channel. Although the flame has become unsteady downstream, the anchor point of the flame is still stable. Fuel injection from the downstream wall of the cavity was also considered for $Re = 1000$. In this case, the combustion efficiency decreased to 22%.

The two-dimensional approximation means that the injected fuel acts as a sheet, rather than a jet. When fuel is injected from the upstream wall of the cavity, the oxygen initially in the cavity is quickly burned and replaced with combustion products. Since the fuel acts as a sheet, inflowing air cannot flow around the fuel into the cavity, but instead must diffuse though the fuel. This limits the locations where fuel and oxidizer can react, lowering the combustion efficiency. Figure 24 shows the temperature contours when additional air is injected from the bottom and downstream walls of the cavity for the case with upstream fuel injection at $Re = 1000$. A secondary flame is established in the cavity and the combustion efficiency increases to 35%.

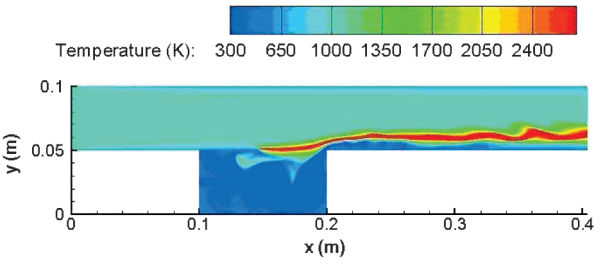

Fig. 23 Fuel injection from the upstream wall at $Re = 2000$.

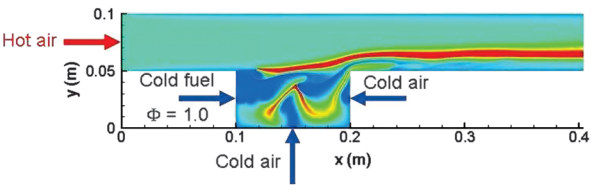

Fig. 24 Fuel injection from the upstream wall with additional air injection at $Re = 1000$.

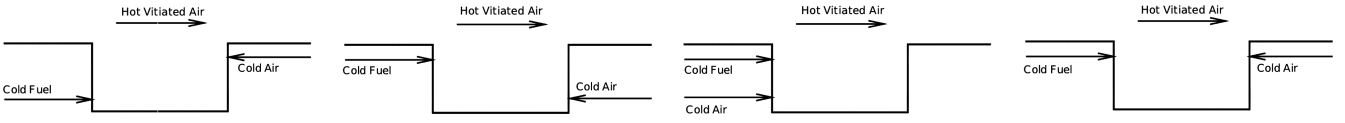

Fig. 25 Injection configurations.

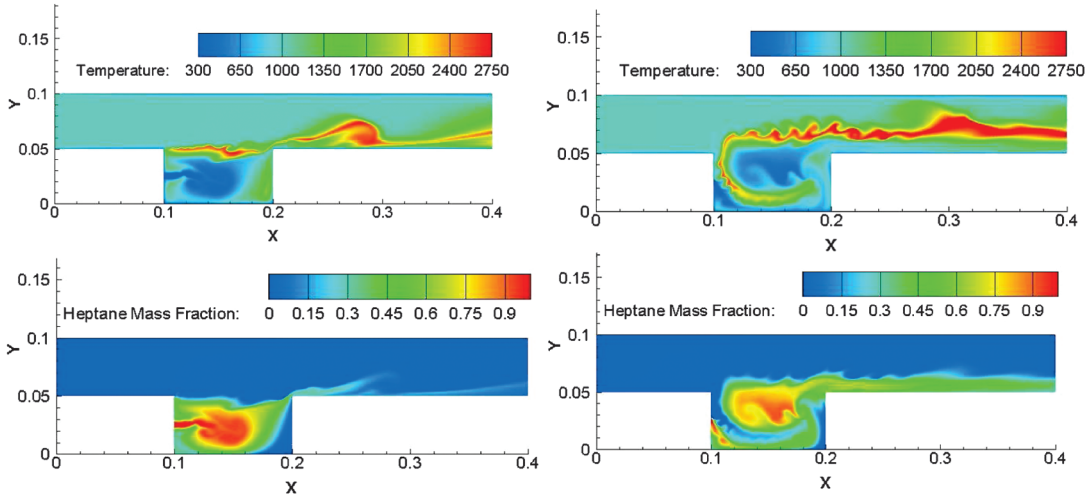

Fig. 26 Temperature and fuel mass fraction contours at a) 0.13 s and b) 0.19 s after igniter is turned off for $Re = 5000$.

We focused our study on four configurations, as indicated in Figs. 25a–25d: disrupting, reinforcing, parallel, and opposing injections. The basic case had 25% of stoichiometry (fuel lean) with 50% vitiated air. The first set of calculations were two-dimensional.

These reacting calculations have been extended to higher Reynolds numbers [69]. Reacting calculations at Reynolds numbers up to 10,000 and cavity aspect ratios of 1 and 2 have been performed with gaseous heptane as the fuel. At higher Reynolds numbers, the entire flame becomes unsteady, including the anchor point. For cavities with an aspect ratio of 1, the flame does not hold in the cavity and is blown downstream for $Re > 5000$. For cavities with an aspect ratio of 2, the flame holds in the cavity at all Reynolds numbers investigated. Temperature and fuel mass fraction contours for $Re = 5000$ are shown in Fig. 26 at two different instants of time. In this case, an igniter has been used between the fuel and airstreams to shorten the calculation time. The igniter is switched off after a flame is established, with the times shown being from when the igniter was turned off. For approximately 0.15 s after the igniter was turned off, the flame remains anchored in the upper upstream corner of the cavity, as shown in the figure. This time corresponds to approximately 4.5 channel residence times. While anchored in this position, the burning efficiency is approximately 85%.

With the two-dimensional approximation, the fuel acts as a sheet or free film, rather than as a round jet, as shown in Fig. 26; so that air from the channel flow cannot easily enter the cavity beneath the fuel stream. However, as shown in Fig. 26b, the fuel stream is deflected downward, allowing air to enter the cavity and the flame to extend around the cavity. Although this increases the air–fuel mixing and the length of the flame, it also displaces unburned fuel from the cavity into the channel and actually reduces the amount of fuel burned. This may be primarily a two-dimensional effect. Three-dimensional calculations are therefore important for this configuration.

The mass flow rate of fuel entering and exiting with time is shown in Fig. 27. Before the initial downward deflection of the fuel stream at approximately 0.15 s, the amount of fuel exiting is relatively constant. After 0.15 s, the fuel mass flow rate at the exit fluctuates considerably as the flow becomes highly unsteady. The mass flow rate of fuel exiting the channel at any instant can be considerably higher than the mass flow rate into the cavity at the same instant. This is the result of the cavity filling with fuel and then being displaced by the inflowing air. After 0.4 s, approximately 12 channel residence times, the flame is still burning in the vicinity of the cavity. The burning efficiency for this calculation is approximately 60%.

The same calculation was performed for a cavity with $L/D = 1.0$. For this square cavity, the flame was blown downstream after less than three channel residence times, so that burning occurred only very near the exit of the channel, resulting in a low burning efficiency of approximately 30%. The calculations were also performed with an inlet Reynolds number of 10,000 for both cavity sizes. The cavity with $L/D = 1$ again had the flame blown downstream, which resulted in a low combustion efficiency of approximately 40%. The longer cavity with $L/D = 2$ showed an improvement in the combustion efficiency over the same cavity at lower Reynolds numbers. The combustion efficiency increased from approximately 60% to 71%. Since the characteristic residence time is inversely proportional to Reynolds number, the increase in combustion efficiency occurs despite the characteristic residence time being halved.

The inlet air temperature for all of these reacting calculations is 1000 K. For $Re < 2000$, the injected gaseous heptane fuel ignited before exiting the channel, establishing a flame that was anchored in the cavity. However, at $Re > 5000$, the fuel did not ignite before exiting and an igniter was switched on until the flame was established. A computation with an extended downstream channel at $Re = 10,000$ shows that ignition occurs approximately 5 channel-heights downstream of the cavity.

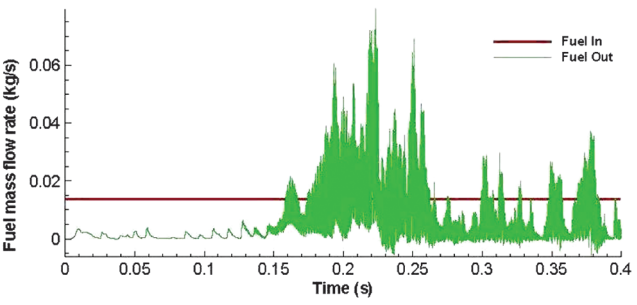

Fig. 27 Fuel mass flow rates for a cavity with $L/D = 2.0$ at $Re = 5000$.

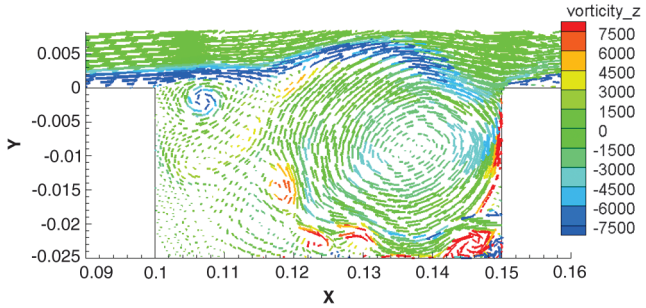

Fig. 28 Reinforcing injection.

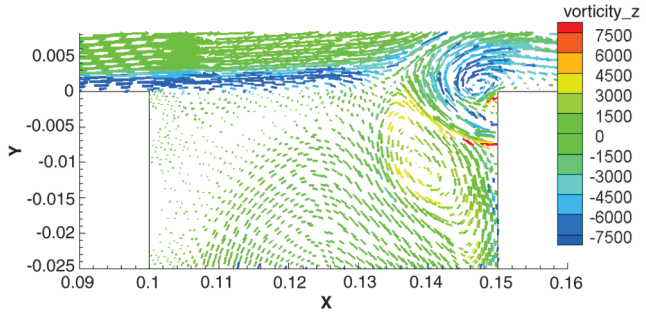

Fig. 29 Disrupting injection.

For all of the reacting calculations, the flowfield becomes much more complex, and there is no clearly identifiable vortex-shedding frequency. Neither Rossiter's formula nor the constant Strouhal number observed for injection without reaction seem to apply when reaction occurs.

For the reinforcing-injection case, as shown in Fig. 28, the lowest burning efficiency was obtained and the large vortices in the cavity were almost stationary. The efficiency becomes modestly higher for the disrupting-injection configuration in Fig. 29. The larger vortex structures are geometrically different from the previous case, but still relatively stationary. In Fig. 30, we see the parallel-injection case, which has much greater unsteady fluctuations and interaction of the vortex structures; the burning efficiency is much higher than for the other cases.

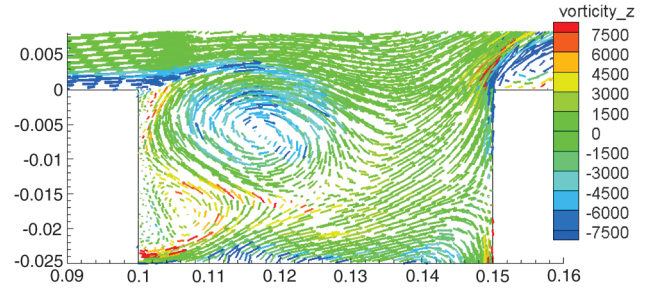

Fig. 30 Parallel injection.

C. Three-Dimensional Reacting Flow Past a Cavity

Three-dimensional, unsteady DNS simulations were made for channel–cavity configurations that were periodic in the spanwise direction. So calculations were made for the flow between two x–y planes: one plane at constant z value passing through the center of the square injector orifice and its jet in the cavity, with the other offjet symmetry plane halfway between two neighboring orifices. (Square holes were used because of their compatibility with a Cartesian mesh.) The three injection configurations shown in Fig. 25 were examined. Figures 31 and 32 show velocity vectors and mixedness contours in the two symmetry planes for disrupting injection and reinforcing injection, respectively.

Velocity vectors and mixedness contours in five y, z planes at different downstream positions are shown in Fig. 33 for the reinforcing-injection case. It is shown that reinforcing injection causes the high-mixedness region to shift upstream compared with the disrupting-injection configuration. Also, the reinforcing-injection case produces the modification of a larger region of the channel flow.

A major difference occurs between the 2-D and 3-D flows. With the slot jet stream for the 2-D case, two portions on opposite sides of the slot jet are disconnected. However, in the 3-D case, there is a flow around each jet stream and between the jets from neighboring orifices. So we can see in Fig. 33 that eddies are created in the third dimension, which will modify the mixing and burning. Smaller length scales are introduced in the 3-D case.

D. Two-Dimensional Reacting Flow Past a Cavity in a Turning Channel

Two-dimensional calculations for cavities in turning channels were performed with a cavity aspect ratio of 4:1 and for parallel- and disrupting-injection configurations. The centerline arc length of the channel was kept the same as the straight-channel case, and the channel was turned through 90 deg. The simulation was repeated with the cavity on the inside and the outside of the curved channel for a Reynolds number of 2000.

Table 2 shows the results on the stability of the four cases considered. With the cavity on the inside the stability does not change in either configuration. Interestingly, with the cavity on the outside, the disrupting case becomes steady while the parallel case becomes

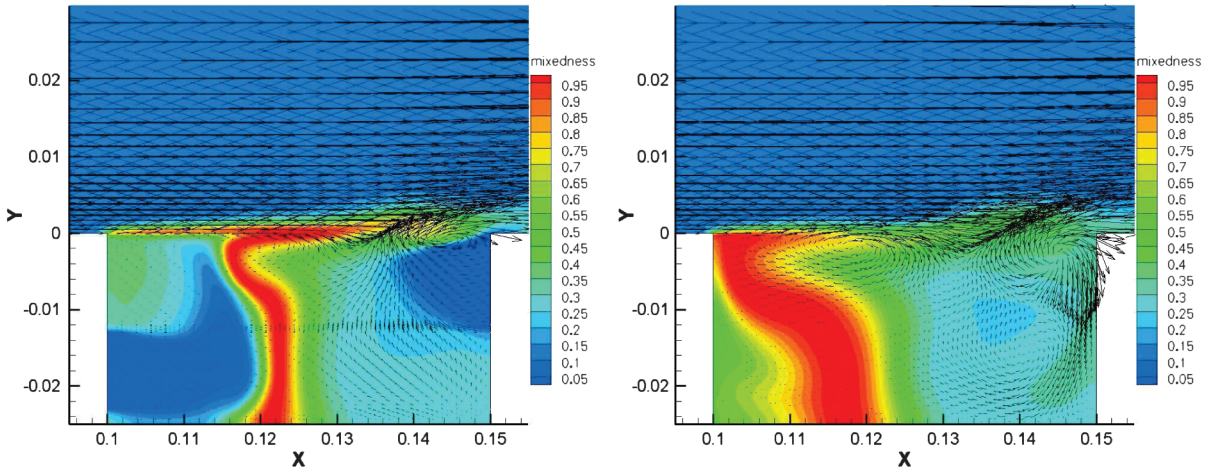

Fig. 31 Three-dimensional reacting flow with disrupting injection into cavity. Side view. $Re = 10,000$ Mixedness contours and velocity vectors: a) jet symmetry plane and b) offjet symmetry plane.

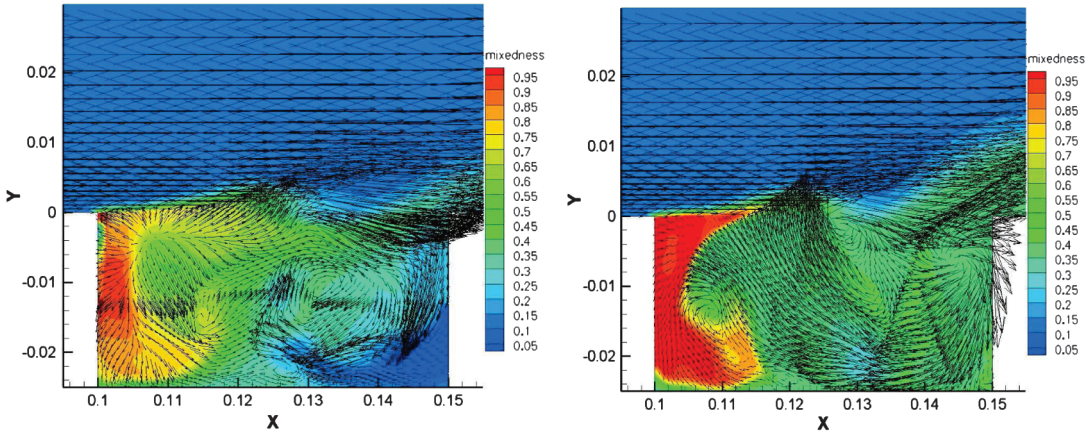

Fig. 32 Three-dimensional reacting flow with reinforcing injection into cavity. Side view. $Re = 10,000$. Mixedness contours and velocity vectors: a) jet symmetry plane and b) offjet symmetry plane.

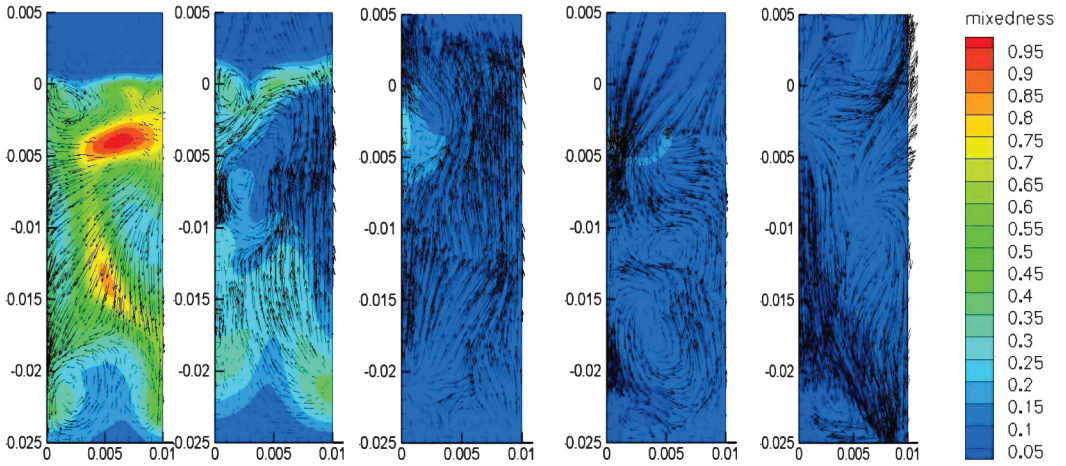

a) x = 0.105 **b) x = 0.115** **c) x = 0.125** **d) x = 0.135** **e) x = 0.145**

Fig. 33 Three-dimensional reacting flow with reinforcing injection into cavity. Cross-sectional slices. $Re = 10,000$. Mixedness contours and velocity vectors.

unsteady. This seemingly contradictory result can be explained by considering the instability mechanisms in effect, as shown in Table 3.

The Kelvin–Helmholtz instability is always present in any channel-cavity flow. The centrifugal instability depends on Rayleigh's circulation criterion [59] for stability:

$$\phi(r) = \frac{1}{r^3}\frac{\mathrm{d}}{\mathrm{d}r}(rV_\theta)^2 \geq 0 \tag{9}$$

Since slip is allowed on the wall opposite the cavity, Fig. 34 shows that with the cavity on the inside of the channel, Rayleigh's criterion is met everywhere. However, with the cavity on the outside, Rayleigh's criterion is not met close to the cavity, so is centrifugally unstable.

The Rayleigh–Taylor instability is present only in the curved-channel cases, since gravitational forces are neglected. However, since the fuel is more dense and the combustion products are less dense than the vitiated air in the channel, it is not known a priori

Table 2 Stability of curving channels

Injection	Straight channel	Cavity on inside	Cavity on outside
Disrupting	Unsteady	Unsteady	Steady
Parallel	Steady	Steady	Unsteady

Table 3 Instability mechanisms in 2-D turning channels

Instability	Straight channel	Cavity on inside	Cavity on outside
Kelvin–Helmholtz	Unstable	Unstable	Unstable
Centrifugal	——	Stable	Unstable
Rayleigh–Taylor	——	Case-dependent	Case-dependent

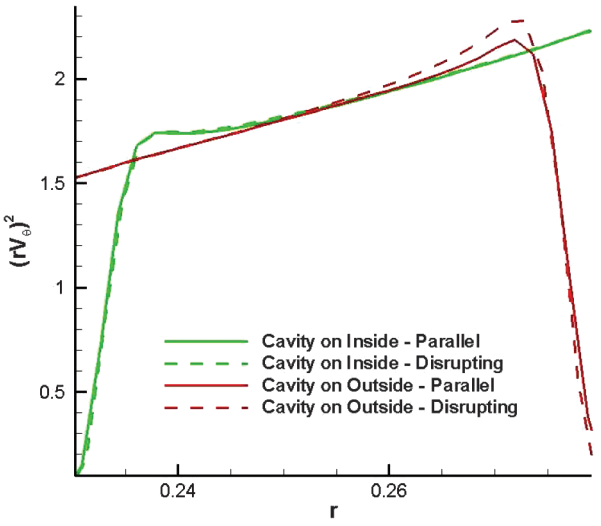

Fig. 34 Centrifugal stability of turning channels.

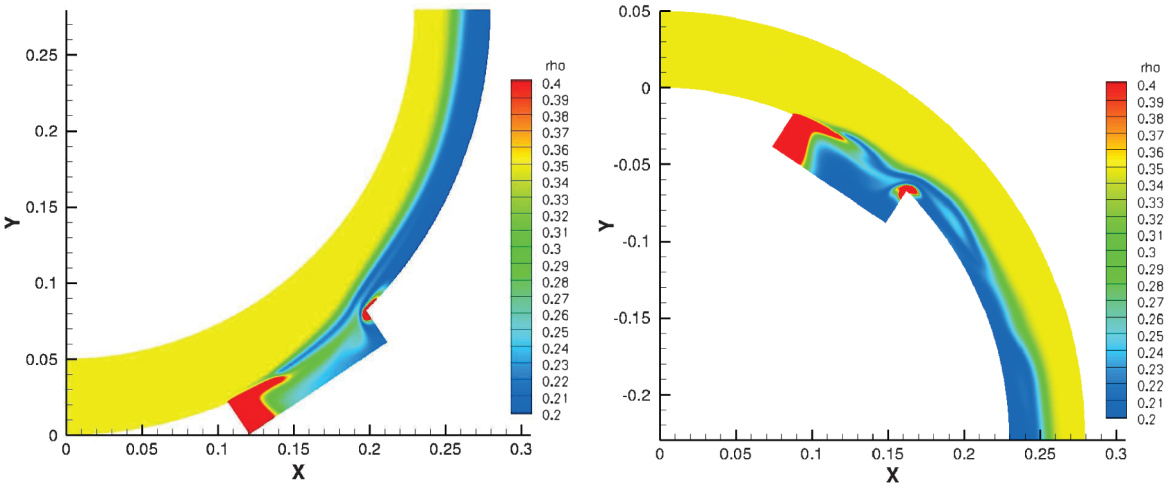

Fig. 35 Density contours for turning channels with disrupting injection.

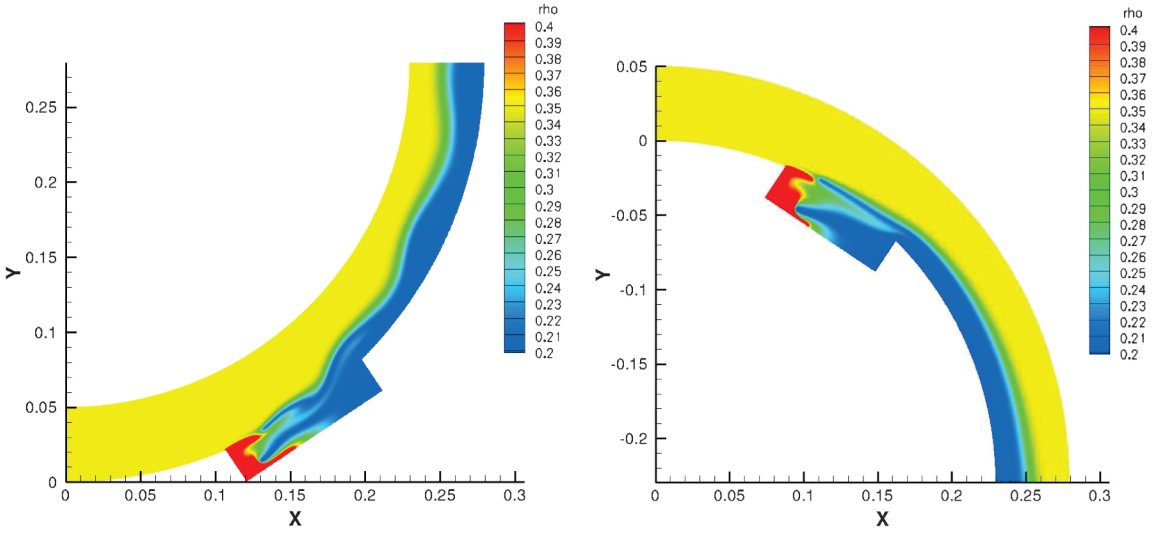

Fig. 36 Density contours for turning channels with parallel injection.

whether the Rayleigh–Taylor instability will be stabilizing or destabilizing. The density contours show that the density in the cavity is affected by the injection configuration. With the disrupting injection, shown in Fig. 35, relatively high-density fluid is injected at both ends of the cavity. This tends to stabilize the case with the cavity on the outside. However, with parallel injection, shown in Fig. 36, all of the high-density fluid is injected at the upstream wall of the cavity and low-density combustion products fill most of the cavity. This makes the case with the cavity on the outside more unstable to Rayleigh–Taylor instabilities.

Figure 37 shows that the stable case with the cavity on the outside also has the highest burning efficiency and mixedness. Because it is steady, a fluid particle spends a longer time in the cavity before being ejected than in unsteady configurations. This leads to a higher mixedness and a higher burning efficiency than unsteady configurations.

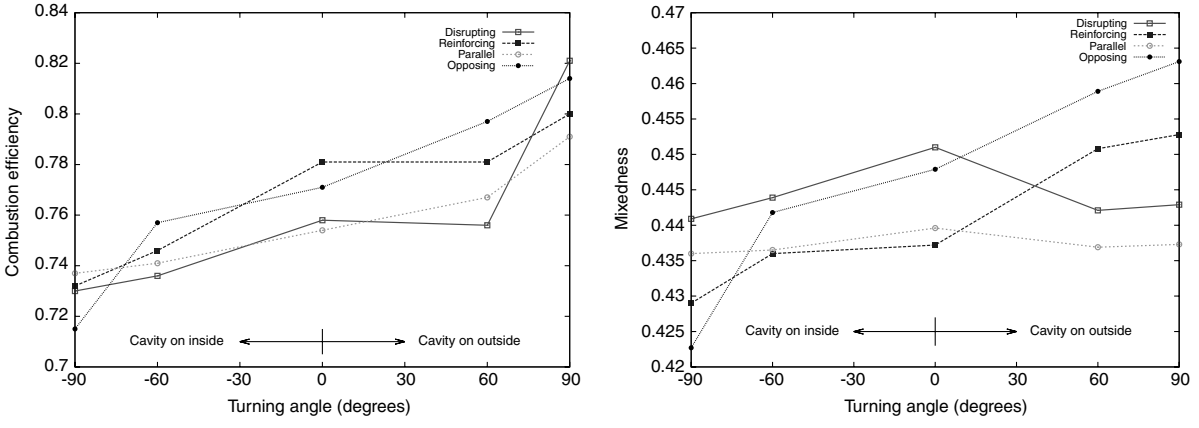

Fig. 37 Efficiencies and mixedness for straight and turning channels.

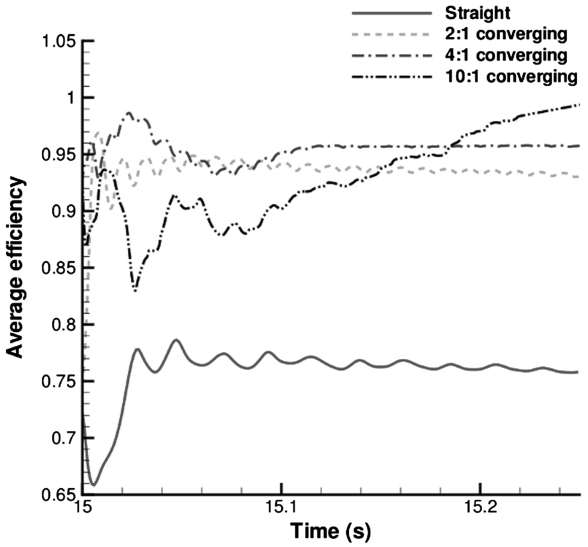

Fig. 38 Efficiencies for straight and converging channels.

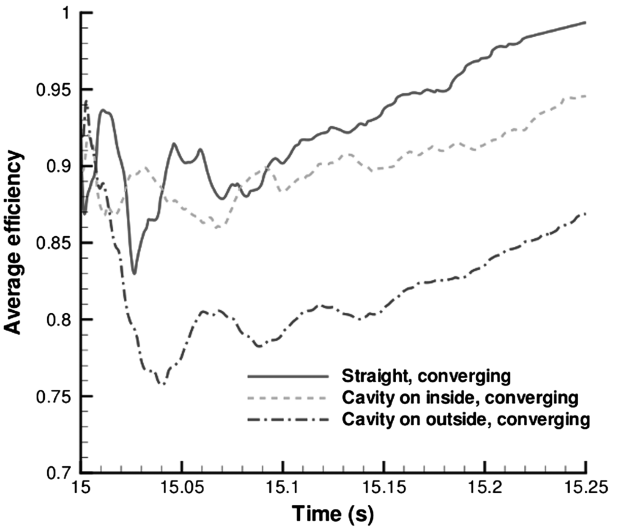

Fig. 40 Efficiencies for converging and turning/converging channels.

E. Two-Dimensional Reacting Flow Past a Cavity in a Converging Channel

Figure 37 shows the efficiencies for straight and converging channels. The efficiency shows an increase with a converging channel, despite the decrease in residence time associated with the acceleration. However, the mixedness tends to decrease with a converging channel, as shown in Fig. 38. The reaction-rate contours for the straight and converging channel are shown in Fig. 39. The converging-channel contours are similar, but structures in the channel are elongated by the acceleration.

F. Two-Dimensional Reacting Flow Past a Cavity in a Turning and Converging Channel

Turning- and converging-channel calculations give results that are similar to the earlier turning-channel and converging-channel results. Figure 40 shows the burning efficiencies for the converging and turning/converging cases. The case with the cavity on the outside wall is stable, as in the nonconverging/turning-channel case, as shown in Fig. 41. One notable difference is that the high-reaction-rate region downstream of the cavity is much smaller in the converging/turning channel than the nonconverging/turning channel.

Stagnation pressure losses have been examined in the case of the converging, turning channel with cavity on the outside. Effects of cavity, injection and mixing, and chemical reaction have been separated and found to be small, collectively about 1% of the entering pressure. At these low Mach numbers, the difference between static and stagnation pressures is less than 1%. The small pressure losses show the promise for the turbine-burner concept.

IX. UCI Experimental Research

To complement the computational findings, experiments were conducted in a high-speed subsonic combustion rig. It was not

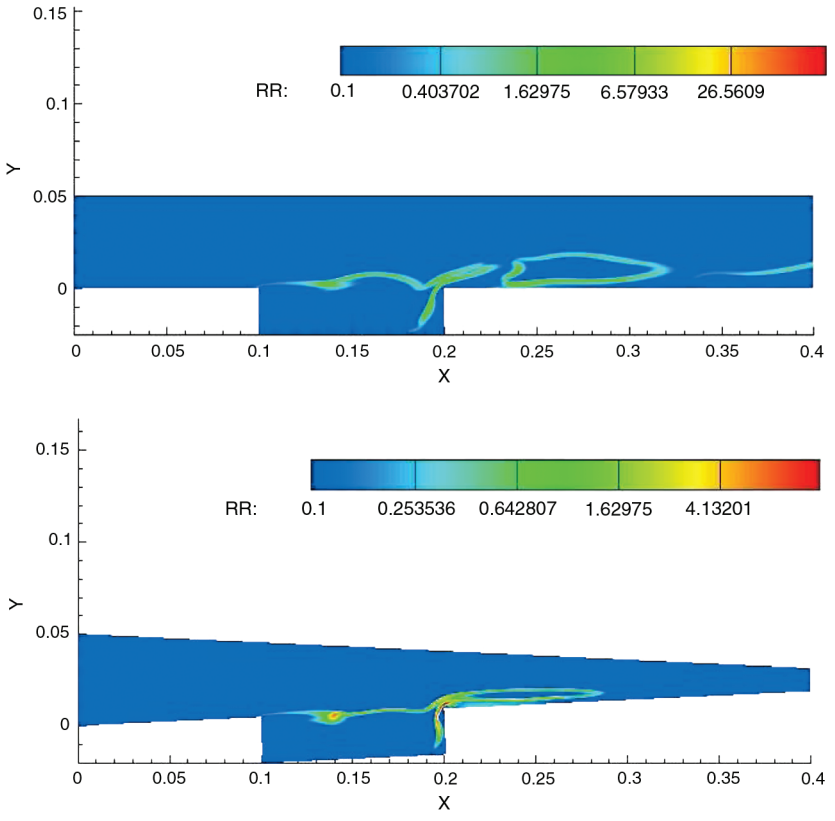

Fig. 39 Reaction-rate contours for straight and converging channels.

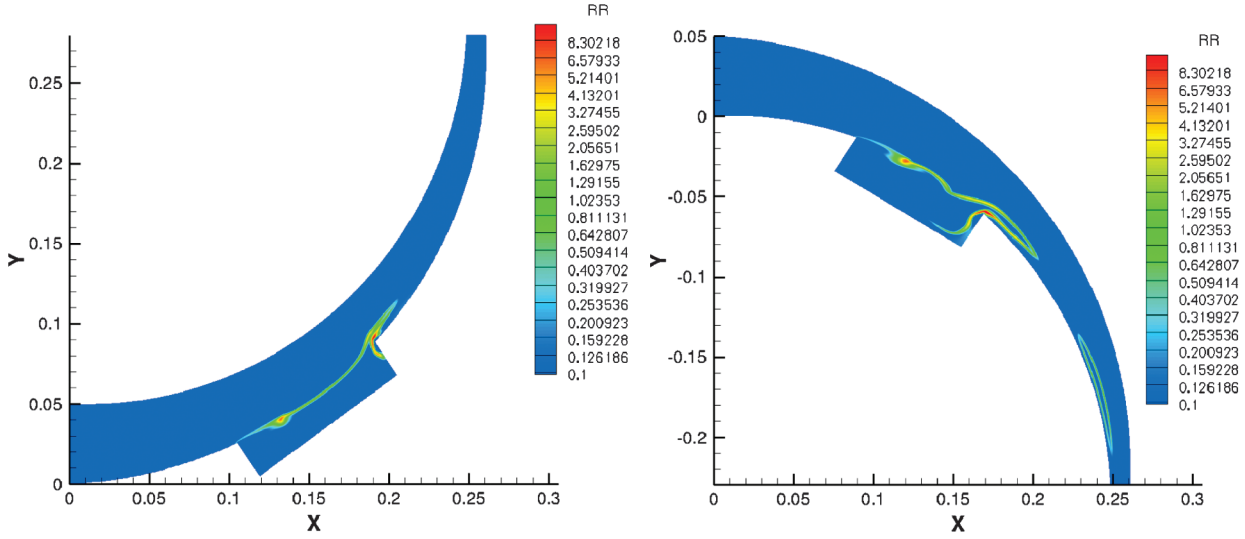

Fig. 41 Reaction-rate contours for turning/converging channels.

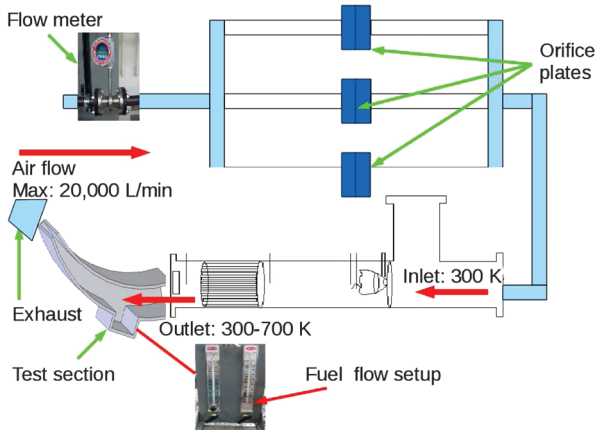

Fig. 42 Experiment layout.

possible to fully match the numerical and experimental conditions, but the major features were retained. Details of the experimental campaign, including nonreacting flow studies and combusting cases with both gaseous and liquid fuels are available in [71–79] spanning three years. Some of the key features of the reacting flow experiments are repeated briefly in the following. Ultimately, the rig (sketched in Fig. 42) had an inlet air system that could provide an air flow rate up to 0.4 m^3/s (24, 000 liters/ min). The airflow was measured using three orifice-plate flow meters, each of which was calibrated for flow rates not exceeding 0.167 m^3/s (8000 liters/ min). The air was straightened using a cylindrical settling chamber of 1.6 m length and 0.4 m in diameter. The exhaust from the test section was captured using a suction system that had the capacity to handle flow rates of 1 m^3/s.

The test section had a rectangular cross section and a constant width of 10 cm. The inlet area was 50 cm^2 and the outlet area was 10 cm^2. The total centerline length of the test section was 30 cm. The cavity center was placed at a point that was 5 cm from the inlet along the centerline. To provide optical access, one wall of the test section and the cavity base had high-temperature glass windows. The flow entering the test section was verified as having a plug-flow profile.

To study the effect of curvature on flame-anchoring, two test sections were used. Both test sections had the same channel curvature and contraction characteristics, as well as the same cavity dimensions and axial location; the only difference was the radial location of the cavity. One test section (Fig. 43a) had the cavity on the inner wall of the channel, and the other test section (Fig. 43b) had the cavity on the outer wall of the channel. The cavity was built such that the cavity depth could be changed. For the experiments described here, deep (5 cm) and shallow (2 cm) cavity depths are included. For each setup, two cavity aspect ratios ($L/D = 1$ and 2.5) were studied.

Fuel injection into the test section was done via the cavity. The fuel was injected at various places to find the optimal location. It was found in the experimental study that the injection location had an effect, albeit limited, on the absolute values of temperatures and burning efficiency, but the qualitative behavior of the flameholding was not affected. Propane and liquid *n*-heptane were used as fuels. The injection location was the same for both liquid and gaseous fuels. For all the results shown here, a spark igniter was used inside the cavity to ignite the fuel. The test section was allowed to reach thermal equilibrium, which took approximately 5–8 minutes from the start of combustion, depending on the volume of fuel being burned.

Flame blowout studies were conducted over a wide range of fuel and air flow rates. The fuel flow rate was kept constant and the airflow rate was increased from zero to blowout. The lean blowout was noted as the highest air flow rate at which the flame just blows out. The rich limit was described by the minimum air flow rate required for

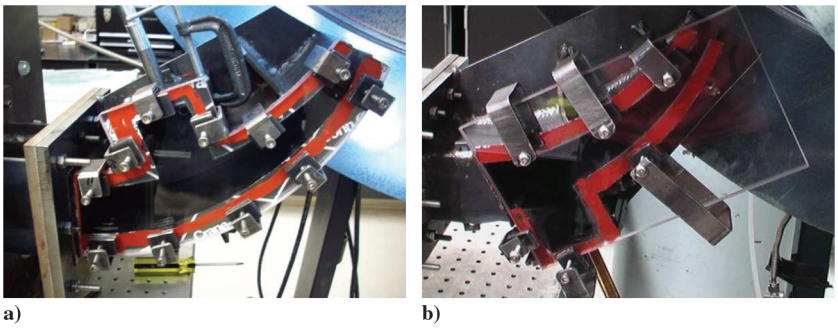

a) b)

Fig. 43 The two test sections with differing cavity locations.

a) b) c)

Fig. 44 Three regimes of combustion.

Table 4 Validity ranges for the combustion regimes

	Aspect ratio	
Cavity location	$L/D = 1$	$L/D = 2.5$
Inner wall	Very low: $Re < 11,000$	Very low: $Re < 6500$
Inner wall	Very high: $Re > 44,500$	Very high: $Re > 28,000$
Outer wall	Very low: $Re < 9800$	Very low: $Re < 5800$
Outer wall	Very high: $Re > 41,000$	Very high: $Re > 29,300$

ignition at a given fuel flow rate. From this study, an interesting qualitative result was observed. As the fuel flow rate was held constant and the air flow rate was increased, it was shown that the combustion inside the cavity went through three distinct regimes. This behavior was shown for both test sections with both shallow- and deep-cavity configurations for gaseous fuels.

As an example, for the test section with the cavity on the inner wall, a deep cavity, and for a fixed propane flow rate of 5×10^{-5} m^3/s, the rich-blowout limit was at $Re = 5000$, and the lean-blowout limit was at $Re = 107,000$. At very low air flow rates ($Re = 5000$–$10,000$), without large turbulent fluctuations, the flame was confined to the shear layer (Fig. 44a). This was expected, as very little air entered the cavity at these flow rates, so the mixture inside the cavity was too rich for combustion, and the residence time of air in the main channel was long enough to facilitate mixing. At high air flow rates ($Re > 40,000$), most of the combustion occurred in the cavity with significant levels of turbulent fluctuations (Fig. 44c). Camera framing rates here were 60 fps. At these air flow rates, the local equivalence ratios inside the cavity were within flammability limits. There was almost no combustion outside the cavity, because the residence times of the airflow outside the cavity were very low (0.012 s) and the global mixture was lean. At moderate air flow rates ($Re = 10,000$–$40,000$), the flame was not stable in the cavity after the igniter was turned off (Fig. 44b). See Table 4 for a summary of configurations and Reynolds numbers for the experiments.

For a fixed fuel flow rate, it was shown that the ranges in which the three regimes occur did not depend on the radial location of the cavity, but depended on the cavity aspect ratio. For shallow cavities the transition occurred at a lower Reynolds numbers, and the unstable regime spanned a smaller range of flow rates, as compared with the deep cavities. The qualitative behavior observed in all cavity configurations suggests that the blowout limits and the regimes of cavity combustion are not strongly dependent on the channel curvature, but depend upon the cavity dimensions and air/fuel flow rates.

To study flame-anchoring mechanisms, CH* chemiluminescence analysis was carried out for all configurations. A high-speed camera was used to capture images of the flame. The charge-coupled-device sensor on the camera was covered by a narrowband filter, 431 ± 10 nm, which limited the radiation to the band where the excited CH* radical is visible. The chemiluminescence is line-of-sight-integrated across the depth of the view field. In addition, there is a broadband contribution from the luminous soot (even in the narrowband-filtered region), so the images shown should be interpreted as being associated with overall reaction, rather than with detailed reaction-zone structures. The bright areas in the images (Figs. 45a and 45b) do, however, represent areas of combustion. From the images it can be shown that there are two distinct regions where combustion takes place: the shear layer and the cavity. The figures also show a linearly expanding shear layer and a cavity where the combustion seems almost uniform. The images also show that the flame in the shear layer is anchored at the upstream edge of the cavity.

Temperature profiles are shown in Fig. 46 for two Reynolds numbers. The image is from the lower $Re = 40,000$ case. At higher Reynolds numbers, the flow is more turbulent, fuel/air mixing is enhanced, and more fuel is burned in the cavity. The fuel flow rate is

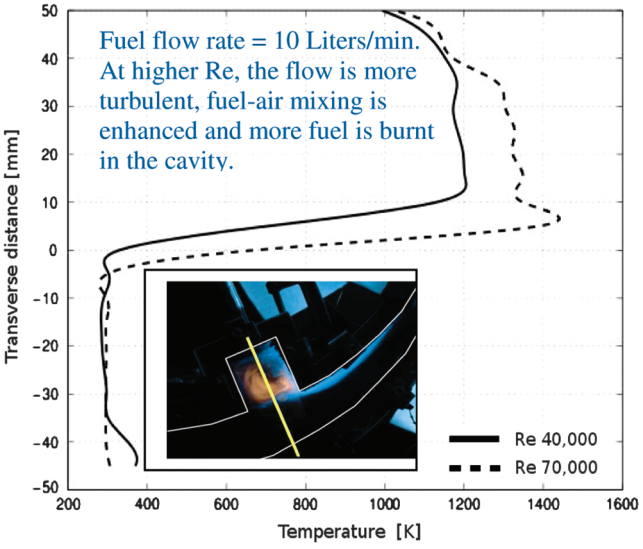

Fig. 46 Temperature profile across the cavity.

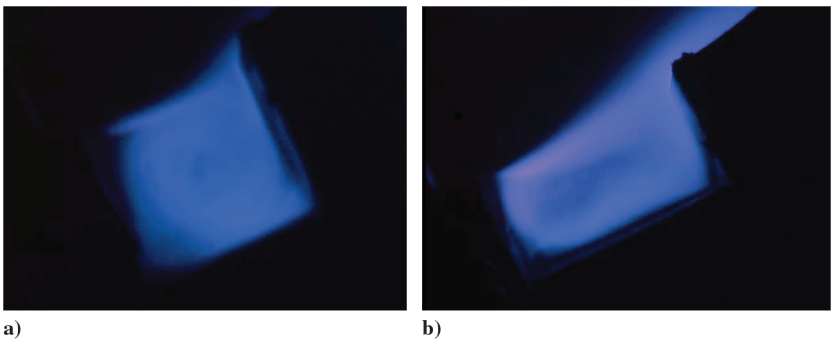

a) b)

Fig. 45 CH* chemiluminescence: a) deep cavity and b) shallow cavity. Framing rate is 5000 fps.

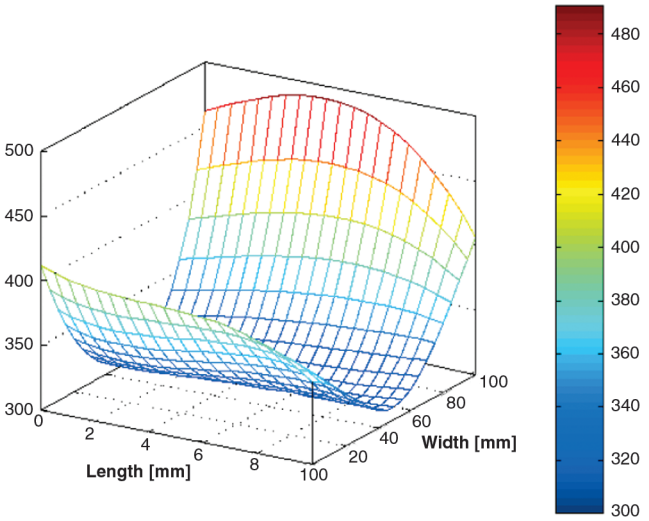

Fig. 47 Flame shape.

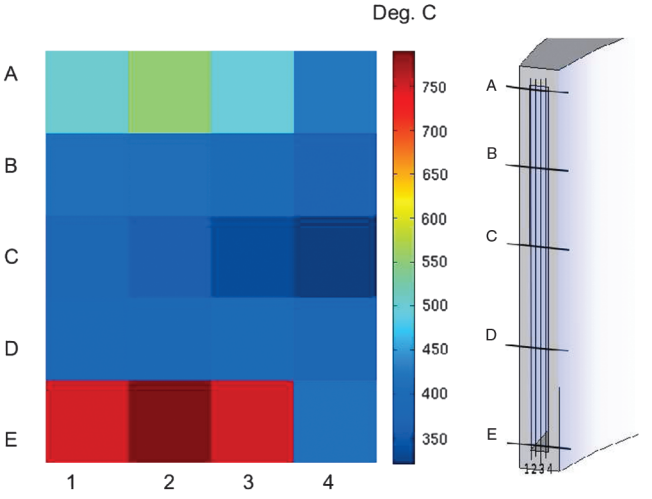

Fig. 49 Temperature profile at cavity exit.

10 liters/ min. The flame wraps near the two sidewalls of the cavity, as shown in Fig. 47. The flame is not symmetric, due to the Pyrex window.

From the experiments, the following observations were made:

1) The combustion in the shear layer was a diffusion flame, where the fuel from inside the cavity diffuses into the air from the channel flow. This behavior was clearly observable at low Reynolds numbers, when the combustion was confined to the shear layer (Fig. 44a).

2) Combustion inside the cavity mimics a well-stirred reactor. The fuel and air mixed and the combustion occurred when the mixture equivalence ratio was within the flammability limits. The combustion was initiated by the heat transferred from the shear layer by convection and radiation. The idea of a stirred reactor was used because the temperature profile inside the cavity is almost uniform, except near the walls. This can be shown in the representative temperature profile (Fig. 46).

3) At higher Reynolds numbers, the percentage of combustion occurring inside the cavity increases and correspondingly the percentage of combustion in the shear layer decreases; this can be shown as a change in relative intensities of the shear layer and the cavity combustion in the narrowband-filtered images (Fig. 48a and 48b).

Temperature profiles were also taken at the exit of the test section using thermocouple type K and correcting for radiation effects. These profiles were taken at 20 points in the exit section. Figure 49 shows the points in the exit section where the temperatures were taken. Figure 49 also shows an example temperature profile at the exit. The profile shows that the temperature at the walls was lower than the temperature at the center of the test section. This was due to the cooling of the walls due to natural and forced convection in the room. The temperature was not uniform at the exit of the test section. It was higher near the inner wall and lower near the outer wall. This was due to the fact that the hot products from the cavity were transported across the channel by centrifugal forces.

The temperature pattern factor at the exit is a measure of the uniformity of the temperature at the exit. Figure 50 shows the temperature pattern factor as a function of inlet Reynolds number. The graph shows that the temperature is more uniform at higher Reynolds numbers. The pattern factor also shows that the temperature is more uniform for all shallow-cavity cases compared with the corresponding deep-cavity cases. This result indicates more robust mixing between the cavity gases and the main flow gases with the unsteady shallow-cavity interaction, as compared with the more stable locked vortex configuration of the deep cavity.

In conclusion for gaseous combustion:

1) There are two distinct combustion zones: the shear layer and the cavity.

2) The shear layer behaves like a diffusion flame and the cavity like a stirred reactor.

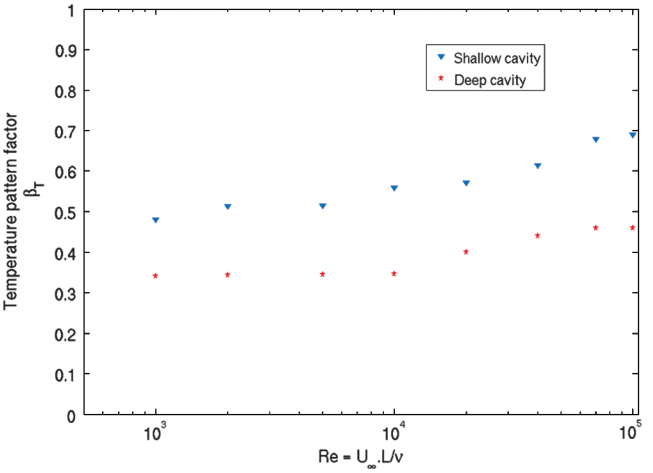

Fig. 50 Temperature pattern factor at the cavity exit.

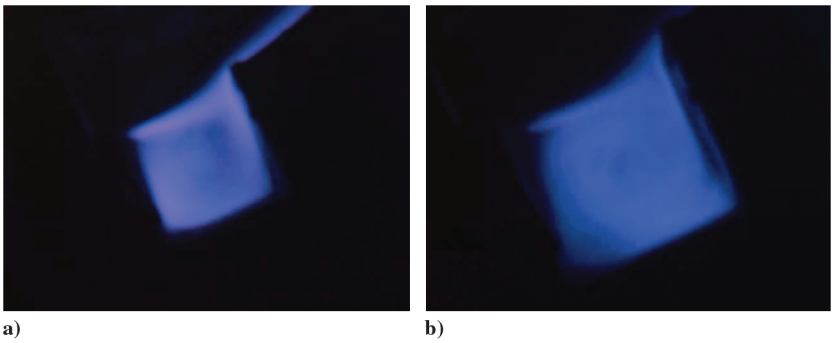

a) **b)**

Fig. 48 CH* chemiluminescence: a) $Re = 40,000$ and b) $Re = 70,000$. Framing rate is 5000 fps.

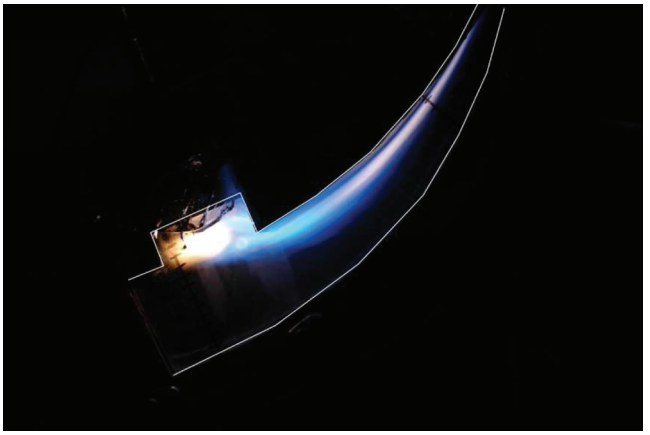

Fig. 51 Liquid-fuel combustion at $Re = 40,000$.

3) The division of overall combustion between the cavity and the shear layer depends on the corresponding mixing time scales. Specifically, the diffusion time scale in the shear layer and the stirred reactor mixing time scale inside the cavity. As the Reynolds number increases, the time available for diffusion into the shear layer decreases at the same time, the amount of air entering the cavity increases, due to the increase in the shear-layer oscillations.

4) The temperature pattern factor at the exit suggests that the mixing of burned gases and the main airflow is more efficient in the shallow-cavity case compared with the deep-cavity case. This result is consistent with the numerical simulation of cavity driven flows.

A few liquid-fuel experiments were also accomplished. An example image is shown in Fig. 51. From observations of liquid-fuel combustion, it was shown that the qualitative behavior for liquid-fuel combustion was very similar to that of gaseous fuel once the experimental setup reached thermal equilibrium. Liquid fuel was injected into the cavity using a simplex injector, which had an injection with an open cone of 70 deg. The injector created a mist of fuel that was ignited by the existing combustion in the system once the system was in thermal equilibrium. The liquid-fuel tests required a propane pilot flame ignited upstream of the cavity to start and sustain the combustion until the test section and the surroundings reached thermal equilibrium. Once thermal equilibrium was achieved, the pilot flame was turned off and the system was self-sustaining. The combustion was more vigorous and for larger fuel flow rates, combustion could not be sustained, but for most of the conditions described in the operational map, liquid-fuel combustion was achieved.

X. Conclusions

The turbine burner holds promise as a major technological advancement for gas-turbine engines. The thermal-cycle analysis for augmentative combustion in the passages of the turbine on a turbojet or turbofan engine shows the potential for large percentage improvements in engine performance. Various types of compact combustors have been studied and can be used as augmentative combustors between turbine stages. These will achieve some performance improvement. Augmentative combustion integrated with the turbine function could achieve even higher performance levels, but the challenges are substantial based on several factors, including millisecond residence times and flow acceleration levels at 10^5 g. The processes of combustion in flows with extremely high levels of streamwise accelerations and turning rates present a new fundamental area of combustion science.

We have several bodies of scientific literature that encourage us to believe that ignition and flameholding is achievable in the high-acceleration flow of a turbine burner: the experimental advances in supersonic combustion; the supporting ignition data, and our own experimental and computational findings. It should be possible with the use of cavities to obtain the necessary residence times. Aeration of the liquid-fuel streams can be helpful. It might be possible to rely on autoignition, due to the hot products and air mixture following through the turbine burner. If not, spark ignition and pilot flames are possibilities.

There has been significant theoretical and computational research on reacting mixing layers in accelerating flows and flameholding in high-speed flows. Three hydrodynamic instabilities are shown to be relevant: Kelvin–Helmholtz instability, Rayleigh–Taylor instability, and the centrifugal instability related to the gradient of angular momentum. Useful work on the stabilization of flames in accelerating and turning flows has taken several other forms: two-dimensional computations for Reynolds-averaged turbulent flow through straight and turning channels; quasi-two-dimensional representations of reacting, converging (and converging/turning) channel flows; and two- and three-dimensional computations for time-dependent transitional flows through passages for cases with and without cavities. Various configurations for injection of fuel and air into the cavity have been examined and compared. Measures for burning efficiency and mixedness have been developed to compare these configurations. The best performance occurs with parallel injection for fuel and air according to the two-dimensional computations. Rossiter modes for the interface flow between the cavity and the channel do not occur for the reacting cases.

Experimental results including flame videos and temperature and chemiluminescence measurements over a wide Reynolds number range have been useful in characterizing the flow. Three combustion regimes have been identified: a low-Reynolds-number regime with the flame in a shear layer, a mid-Reynolds-number regime with a shear-layer flame and an intermittent flame in the cavity, and a high-Reynolds-number domain with a stable cavity flame. Cavity placements on the inside and outside of the turn show some differences. Effects of the cavity length and depth, injection orientation for fuel and air into the cavity, passage turning radius, and Reynolds number magnitude have been identified.

Work in the near future will yield more computations with curved and converging channels with fuel and air injection into the cavity. Experiments and computations are needed with choked exit nozzle, higher pressures in the channel, and liquid-fuel injection into the cavity. Better understanding of flameholding, mixing efficiency, and burning efficiency in these configurations is the goal.

Acknowledgments

The authors wish to thank the U.S. Air Force Office of Scientific Research for supporting this research through grant FA 9550-06-1-0194 with Julian Tishkoff as the Scientific Officer. Joseph Zelina of the U.S. Air Force Research Laboratory is also thanked for his advice.

References

[1] Sirignano, W. A., and Liu, F., "Performance Increases for Gas Turbine Engines Through Combustion Inside the Turbine," *Journal of Propulsion and Power*, Vol. 15, Jan.–Feb. 1999, pp. 111–118. doi:10.2514/2.5398

[2] Liu, F., and Sirignano, W. A., "Turbojet and Turbofan Engine Performance Increases Through Turbine Burners," *Journal of Propulsion and Power*, Vol. 17, 2001, pp. 695–705. doi:10.2514/2.5797; also AIAA Paper 2000-0741, Jan. 2000.

[3] Chen, G., Hoffman, M., and Davis, R., "Gas-Turbine Performance Improvements Through the Use of Multiple Turbine Interstage Burners," *Journal of Propulsion and Power*, Vol. 20, No. 5, Sept.–Oct. 2004, pp. 828–834. doi:10.2514/1.2886

[4] Liew, K. H., Urip, E., and Yang, S. L., "Parametric Cycle Analysis of a Turbofan Engine with an Interstage Turbine Burner," *Journal of Propulsion and Power*, Vol. 21, No. 3, May–June 2005, pp. 546–551. doi:10.2514/1.2546

[5] Lin, K.-C., Kirdendall, K. A., Kennedy, P. J., and Jackson, T. A., "Spray Structures of Aerated Liquid Fuel Jets in Supersonic Crossflows," 35th Joint Propulsion Specialists Meeting, AIAA Paper 99-2374, 1999.

[6] Lin, K.-C., Kennedy, P. J., and Jackson, T. A., "Spray Penetration Heights of Angle-Injected Aerated-Liquid Jets in Supersonic Crossflows," Aerospace Sciences Meeting, AIAA Paper 2000-0194, 2000.

[7] Hsu, K.-Y., Carter, C., Crafton, J., Gruber, M., Donbar, J., Mathur, T., Schommer, D., and Terry, W., "Fuel Distribution About a Cavity Flameholder in Supersonic Flow," 36th Joint Propulsion Specialists Meeting, AIAA Paper 2000-3585, 2000.
[8] Mathur, T., Cox-Staufer, S., Hsu, K.-Y., Crafton, J., Donbar, J., and Gruber, M., "Experimental Assessment of a Fuel Injector for Scramjet Applications," 36th Joint Propulsion Specialists Meeting, AIAA Paper 2000-3703, 2000.
[9] Gruber, M., Donbar, J., Jackson, T., Mathur, T., Eklund, D., and F. Billig, F., "Performance of an Aerodynamic Ramp Fuel Injector in a Scramjet Combustor," 36th Joint Propulsion Specialists Meeting, AIAA Paper 2000-3708, 2000.
[10] Mathur, T., Lin, K.-C., Kennedy, P. J., Gruber, M., Donbar, J., Jackson, T., and Billig, F., "Liquid JP-7 Combustion in a Scramjet Combustor," 36th Joint Propulsion Specialists Meeting, AIAA Paper 2000-3581, 2000.
[11] Yu, G., Li, J. G., Chang, X. Y., and Chen, L. H., "Investigation of Fuel Injection and Flame Stabilization in Liquid Hydrocarbon-Fueled Supersonic Combustors," 37th Joint Propulsion Conference, AIAA Paper 2001-3608, 2001.
[12] Yu, G., Li, J. G., Chang, X. Y., Chen, L. H., Sung, C. J., "Investigation on Combustion Characteristics of Kerosene Hydrogen Dual Fuel in a Supersonic Combustor," 36th Joint Propulsion Specialists Meeting, AIAA Paper 2000-3620, 2000.
[13] Glassman, I., *Combustion*, 3rd ed., Academic Press, New York, 1996, pp. 589–603.
[14] Spadaccini, L. J., and Colket, M. B., III, "Ignition Delay Characteristics of Methane Fuels," *Progress in Energy and Combustion Science*, Vol. 20, 1994, pp. 373–460. doi:10.1016/0360-1285(94)90010-8
[15] Billing, F. S., "Research on Supersonic Combustion," *Journal of Propulsion and Power*, Vol. 9, No. 4, 1993, pp. 499–514. doi:10.2514/3.23652
[16] Abbitt, J., Segal, C., McDaniel, J. C., Cross, R. H., and Whitehurst, R. B., "Experimental Supersonic Hydrogen Combustion Employing Staged Injection Behind a Rearward-Facing Step," *Journal of Propulsion and Power*, Vol. 9, No. 3, 1993, pp. 472–478. doi:10.2514/3.23646
[17] Tishkoff, J. M., Drummond, J. P., Edwards, T., and Nejad, A. S., "Future Direction of Supersonic Combustion Research," AIAA Paper 97-1017, Jan. 1997.
[18] Ben-Yakar, A., and Hanson, R. K., "Cavity Flame-Holders for Ignition and Flame Stabilization in Scramjets: An Overview," *Journal of Propulsion and Power*, Vol. 17, No. 4, 2001, pp. 869–877. doi:10.2514/2.5818
[19] Lapsa, A., and Dahm, W. J. A., "Experimental Study on the Effects of Large Centrifugal Forces on Step-Stabilized Flames," *5th U. S. Combustion Meeting*, March 2007.
[20] Shouse, D. T., Hendricks, R. C., Burrus, D. L., Roquemore, W. M., Ryder, R. C., Duncan, B. S., Liu, N.-S., Brankovic, A., Hendricks, J. A., and Gallagher, J. R., "Experimental and Computational Study of Trapped Vortex Combustor Sector Rig with Tri-Pass Diffuser," NASA John H. Glenn Research Center, Cleveland, OH, Jan. 2004.
[21] Sturgess, G. J., Zelina, J., Shouse, D. T., Roquemore, W. M., "Emissions Reduction Technologies for Military Gas Turbine Engines," *Journal of Propulsion and Power*, Vol. 21, No. 2, 2005, pp 193–217. doi:10.2514/1.6528
[22] Bunker, R. S., "Integration of New Aero-thermal and Combustion Technologies with Long-Term Design Philosophies for Gas Turbine Engines," *US Ukrainian Workshop on Innovative Combustion and Aerothermal Technologies in Energy and Power Systems*, May 2001.
[23] Stone, C., and Menon, S., "Simulation of Fuel/Air Mixing and Combustion in a Trapped Vortex Combustor," 38th AIAA Aerospace Sciences Meeting and Exhibit, Reno, NV, AIAA Paper 2000-478, Jan. 2000.
[24] Steele, R. C., Kendrick, D. W., Chenevert, B. C., Bucher, J., Edmonds, R. G., and Malte, P. C., "The Development of a Lean-Premixed Trapped Vortex Combustor," *Proceedings of ASME Turbo Expo 2003 Power for Land, Sea, and Air*, July 2003.
[25] Singhal, A., and Ravikrishna, R. V., "Single Cavity Trapped Vortex Combustor Dynamics. Part 1: Experiments," *International Journal of Spray and Combustion Dynamics*, Vol. 3, No. 1, 2011, pp. 23–44. doi:10.1260/1756-8277.3.1.23
[26] Singhal, A., and Ravikrishna, R. V., "Single Cavity Trapped Vortex Combustor Dynamics. Part 2: Simulations," *International Journal of Spray and Combustion Dynamics*, Vol. 3, No. 1, 2011, pp. 45–62. doi:10.1260/1756-8277.3.1.45
[27] Zelina, J., Shouse, D. T., and Hancock, R. D., "Ultra-Compact Combustors for Advanced Gas Turbine Engines," ASME IGTI 2004-GT-53155, 2004.
[28] Shouse, D. T., Zelina, J., and Hancock, R. D., "Operability and Efficiency Performance of Ultra-Compact, High Gravity (g) Combustor Concepts," *International Gas Turbine and Aeroengine Congress and Exposition*, May 2006.
[29] Zelina, J., Sturgess, G. J., and Shouse, D. T., "The Behavior of an Ultra-Compact Combustor (UCC) Based on Centrifugally-Enhanced Turbulent Burning Rates," AIAA Paper 2004-3541.
[30] Zelina, J., "Numerical Studies on Cavity-Inside-Cavity-Supported in Ultra Compact Combustors," *Proceedings of ASME Turo Expo 08: 53rd ASME International Gas Turbine and Aeroengine Congress and Exposition*, June 2008.
[31] Anthenien, R. A., Mantz, R. A., Roquemore, W. M., and Sturgess, G. J., "Experimental Results for a Novel, High Swirl, Ultra Compact Combustor for Gas Turbine Engines," *2nd Joint Meeting of the U.S. Sections of the Combustion Institute*, Oakland, CA March 2001.
[32] Zelina, J., Ehret, J., Hancock, R. D., Shouse, D. T., Sturgess, G. J., and Roquemore, W. M., "Ultra-Compact Combustion Technology Using High Swirl to Enhance Burning Rate," AIAA Paper 2002-3725, 2002.
[33] Zelina, J., Sturgess, G. J., Mansour, A., and Hancock, R. D., "Fuel Injection Design for Ultra-Compact Combustor," ISABE Paper 2003-1089, 2003.
[34] Newby, R. A., Bachovchin, D. M., and Lippert, T. E., "Gas Turbine Reheat Using In-Situ Combustion," Siemens Westinghouse Power Corp., May 2004.
[35] Marble, F. E., and Adamson, T. C., Jr., "Ignition and Combustion in a Laminar Mixing Zone," *Jet Propulsion*, Vol. 24, 1954, p. 85.
[36] Emmons, H. W., "Thin Film Combustion of Liquid Fuel," *ZAMM*, Vol. 36, 1956, p. 60. doi:10.1002/zamm.19560360105
[37] Chung, P. M., "Chemically Reacting Nonequilibrium Boundary Layers," *Advances in Heat Transfer*, edited by J. P. Hartnett, and T. F. Irvine, Jr., Academic Press, New York, 1965, pp. 109–270.
[38] Sharma, O. P., and Sirignano, W. A., "On the Ignition of a Pre-Mixed Fuel by a Hot Projectile," *Combustion Science Technology*, Vol. 1, 1970, pp. 481–494. doi:10.1080/00102206908952228
[39] Patankar, S. V., and Spalding, D. B., *Heat and Mass Transfer in Boundary Layers*, Intertext, London, 1970.
[40] Givi, P., Ramos, J. I., and Sirignano, W. A., "Probability Density Function Calculations in Turbulent Chemically Reacting Round Jets, Mixing Layers and One-Dimensional Reactors," *Journal of Non-equilibrium Thermodynamics*, Vol. 10, 1985, pp. 75–104.
[41] Buckmaster, J., Jackson, T. L., and Kumar, A. (eds.), *Combustion in High-Speed Flows*, Kluwer Academic, Dordrecht, The Netherlands, 1994.
[42] Grosch, C. E., and Jackson, T. L., "Ignition and Structure of a Laminar Diffusion Flame in a Compressible Mixing Layer with Finite Rate Chemistry," *Physics of Fluids A*, Vol. 3, 1991, pp. 3087–3097. doi:10.1063/1.857853
[43] Jackson, T. L., and Hussaini, M. Y., "An Asymptotic Analysis of Supersonic Reacting Mixing Layers," *Combustion Science Technology*, Vol. 57, 1988, p. 129. doi:10.1080/00102208808923948
[44] Im, H. G., Chao, B. H., Bechtold, J. K., and Law, C. K., "Analysis of Thermal Ignition in the Supersonic Mixing Layer," *AIAA Journal*, Vol. 32, 1994, pp. 341–349. doi:10.2514/3.11990
[45] Im, H. G., Helenbrook, B. T., Lee, S. R., and Law, C. K., "Ignition in the Supersonic Hydrogen/Air Mixing Layer with Reduced Reaction Mechanisms," *Journal of Fluid Mechanics*, Vol. 322, 1996, pp. 275–96.
[46] Chakraborty, D., Upadhyaya, H. V. N., Paul. P. J., and Mukunda, H. S., "A Thermo-Chemical Exploration of a Two-Dimensional Reacting Supersonic Mixing Layer," *Physics of Fluids*, Vol. 9, No. 11, 1997, pp. 3513–3522. doi:10.1063/1.869459
[47] Li, T. Y., and Nagamatsu, H. T., "Similar Solutions of Compressible Boundary Layer Equations," *Journal of the Aeronautical Sciences*, Vol. 20, 1953, p. 653.
[48] Cohen, C. B., "Similar Solutions of Compressible Laminar Boundary Layer Equations," *Journal of the Aeronautical Sciences*, Vol. 21, 1954, p. 281.
[49] Cohen, C. B., and Reshotko, E., "The Compressible Laminar Boundary Layer with Heat Transfer and Arbitrary Pressure Gradient," NACA Rept. 1294, 1956.
[50] Illingworth, C. R., "Steady Flow in the Laminar Boundary Layer of a Gas," *Proceedings of the Royal Society of London, Series A*, Vol. 199, 1949, p. 533.

doi:10.1098/rspa.1949.0153
[51] Stewartson, K., "Correlated Compressible and Incompressible Boundary Layers," *Proceedings of the Royal Society of London, Series A: Mathematical and Physical Sciences*, Vol. 200, 1949, p. 84. doi:10.1098/rspa.1949.0160
[52] Schlichting, H., *Boundary Layer Theory*, McGraw–Hill, New York, 1979, pp. 340–352.
[53] Sirignano, W. A., and Kim, I., "Diffusion Flame in a Two-Dimensional Accelerating Mixing Layer," *Physics of Fluids*, Vol. 9, 1997, pp. 2617–2630. doi:10.1063/1.869378
[54] Fang, X., Liu, F., and Sirignano, W. A., "Ignition and Flame Studies for an Accelerating Transonic Mixing Layer," *Journal of Propulsion and Power*, Vol. 17, No. 5, Sept.–Oct. 2001, pp. 1058–1066. doi:10.2514/2.5844
[55] Mehring, C., Liu, F., and Sirignano, W. A., "Ignition and Flame Studies for a Turbulent Acceleration Transonic Mixing Layer," 39th Aerospace Sciences Meeting, AIAA Paper 2001-1096, Reno, NV, Jan. 2001.
[56] Cai, J., Icoz, O., Liu, F., and Sirignano, W. A., "Ignition and Flame Studies for Turbulent Transonic Mixing in a Curved Duct Flow," 39th Aerospace Sciences Meeting, AIAA Paper 2001-0189, Reno, NV, Jan. 2001.
[57] Cai, J., Icoz, O., Liu, F., and Sirignano, W. A., "Combustion in a Transonic Turbulent Flow with Large Axial and Transverse Pressure Gradients," *18th ICDERS*, Seattle, WA, July 30–Aug. 3 2001.
[58] Cheng, F., Liu, F., and Sirignano, W. A., "Nonpremixed Combustion in an Accelerating Transonic Flow Undergoing Transition," *AIAA Journal*, Vol. 45, 2007, pp. 2935–2946. doi:10.2514/1.31146
[59] Cheng, F., Liu, F., and Sirignano, W. A., "Nonpremixed Combustion in an Accelerating Turning, Transonic Flow Undergoing Transition," *AIAA Journal*, Vol. 46, 2008, pp. 1204–1215. doi:10.2514/1.35209
[60] Cheng, F., Sirignano, W. A., and Liu, F., "Reacting Mixing-Layer Computations in a Simulated Turbine-Stator Passage," *Journal of Propulsion and Power*, Vol. 25, No. 2, 2009, pp. 322–334. doi:10.2514/1.37739
[61] Drazin, P. G., and Reid, W. H., *Hydrodynamic Instability*, Cambridge University Press, Cambridge, England, U.K., 1981.
[62] Quaale, R. J., Anthenien, R. A., Zelina, J., and Ehret, J., "Flow Measurements in a High Swirl Ultra Compact Combustor for Gas Turbine Engines," ISABE Paper 2003-1141.
[63] Zelina, J., Shouse, D. T., and Hancock, R. D., "Ultra-Compact Combustors for Advanced Gas Turbine Engines," ASME Turbo Expo '04, Paper 2004-GT-53155, 2004.
[64] Zelina, J., Sturgess, G. J., Mansour, A., and Hancock, R. D., "Fuel Injection Design Optimization for an Ultra-Compact Combustor," ISABE Paper 2003-1089, 2003.
[65] Rossiter, J. E., *Wind Tunnel Experiments on the Flow over Rectangular Cavities at Subsonic and Transonic Speeds*, Royal Aircraft Establishment, London, 1964.
[66] Gharib, M., and Roshko, M., "The Effect of Flow Oscillations on Cavity Drag," *Journal of Fluid Mechanics*, Vol. 177, 1987, pp. 501–530. doi:10.1017/S002211208700106X
[67] Colcord, B. J., and Sirignano, W. A., "Combustion Model with Fuel Injection into and Air Flow Past a Cavity," *Proceedings of the Fall Meeting of the Western States Section of the Combustion Institute*, Livermore, CA, Oct. 16–17 2007.
[68] Sarzi-Amade, N., "Preliminary Studies on a Model Turbine Burner," M.S. Thesis, University of California, Irvine, Irvine, CA, 2007.
[69] Colcord, B. J., and Sirignano, W. A., "Combustion in a Flow Cavity," *Proceedings of 5th US Combustion Meeting*, San Diego, CA, March 25–28 2007.
[70] Westbrook, C. K., and Dryer, F. L., "Simplified Reaction Mechanisms for the Oxidation of Hydrocarbon Fuels in Flames," *Combustion Science and Technology*, Vol. 27, 1981, pp. 31–43. doi:10.1080/00102208108946970
[71] Puranam, V., Arici, J., Amade-Sarzi, N., Dunn-Rankin, D., and Sirignano, W. A., "Turbulent Combustion in a Curving, Contracting Channel with a Cavity Stabilized Flame," *Proceedings of the Combustion Institute*, Vol. 32, 2009, pp. 2973–2981. doi:10.1016/j.proci.2008.06.161
[72] Amade, N., Dunn-Rankin, D., and Sirignano, W. A., "Fuel/Air Mixing in a Model Turbine Burner Section," *U.S. Combustion Meeting*, Paper E02, San Diego, March 25–28 2007.
[73] Puranam, S., Sarzi-Amade, N., and Dunn-Rankin, D., "Turbulent Combustion Studies in a Model Turbine Burner," *21st International Colloquium on Dynamics of Explosions and Reactive Systems*, Poitiers, France, July 23–27 2007.
[74] Puranam, S., Colcord, B., Arici, J., Dunn-Rankin, D., and Sirignano, W. A., "Experimental and Numerical Investigation of a Model Turbine-Burner," Western States Section/The Combustion Institute Spring Meeting, Paper 08S-41, March 17–18 2008.
[75] Sirignano, W. A., Dunn-Rankin, D., Liu, F., Colcord, B., and Puranam, S., "Turbine Burners: Flameholding in Accelerating Flow," AIAA Joint Propulsion Conf.AIAA Paper 2009-5410, Denver, CO, Aug. 2–5 2009.
[76] Puranam, S. V., and Dunn-Rankin, D., "Turbulent Combustion in Cavity Stabilized Accelerating Flows," Western States Section/The Combustion Institute Fall Meeting, Paper 09F-19, Oct. 26–27 2009.
[77] Arici, J., Puranam, S. V., Colcord, B., Dunn-Rankin, D., and Sirignano, W. A.,"W4P143: Combustion and Flame Holding in a Turbine Burner Configuration: An Experimental and Numerical Exploration of Reacting Flow in a Curving Contracting Channel," Poster Session of the *32nd International Combustion Symposium*, Montreal, Aug. 3–9 2008.
[78] Puranam, V. S., "Combustion in Cavities and Accelerating Flows," Ph.D. Dissertation, University of California, Irvine, Irvine, CA, 2010.
[79] Amade-Sarzi, N., "Mixing Flows in a Converging Curved Duct," M.S. Thesis, University of California, Irvine, Irvine, CA, 2007.

P. Givi
Associate Editor